83p.

N64-15192
CODE-1
CR-55638

[redacted]

OTS PRICE

XEROX $ 8.10 ph.

MICROFILM $ 2.69 mf.

Alkaline Battery Division

GULTON INDUSTRIES, INC.

Metuchen, N. J.

DESIGN, DEVELOPMENT AND MANUFACTURE OF STORAGE BATTERIES FOR FUTURE SATELLITES

Quarterly ... No. 10, 4 Feb. – 4 Jun. 1963

Report No. 10

NATIONAL AERONAUTICS AND SPACE ADMINISTRATION - NASA CONTRACT NO. NAS 5-809

(NASA CR-55638) OTS:

TENTH QUARTERLY PROGRESS REPORT

4 February 1963 to 4 June 1963

Prepared By:

H. N. Seiger
Asst. Dir. of Research

H. Cohen
Research Chemist

A. Lyall
Chemical Engineer

Approved By:

R. C. Shair
Director of Research

GULTON INDUSTRIES, INC.
Alkaline Battery Division
Metuchen, New Jersey.

TABLE OF CONTENTS

TABLE OF CONTENTS
(continued)

LIST OF TABLES

LIST OF FIGURES

LIST OF FIGURES
(continued)

REFERENCES

1. Gulton Industries, 9th. Monthly Progress Report WADD Contract No. AF 33(600)-41670, May, 1961.

2. Gulton Industries, 9th. Monthly Progress Report, WADD Contract No. AF 33(600)-41670, March, 1962.

3. E. Kantner, Unpublished Work in the Laboratory.

4. Gulton Industries, Nickel-Cadmium Batteries, Technical Documentary Report No. ASD-TDR-62-67, April, 1962.

5. H. Dehmelt and K. von Dohren, Proc. 13th. Annual Power Sources Conference, P. 85, 1959.

6. H. N. Seiger and R. C. Shair, Proc. 15th. Annual Power Sources Conference.

7. S. Yoshizawa & Z. Takehara, Electrochim. Acta, 5, 240 (1961)

8. P. Ives and G. Jang, Reference Electrodes, Academic Press, New York, 1961.

9. Z. Szklarska - Smiolowska and M. Smialowski; J. Electrochem. Soc. 110, 444 (1963).

10. J. Wells, J. Am. Chem. Soc; 33, 504 (1911)

11. H. N. Seiger and R. C. Shair; Paper presented at the Electrochemical Society Meeting, Detroit, Oct. 1961.

12. Gulton Industries, Final Report, S. C. Contr. No. DA 36-039 SC-8539, June 1962.

13. M. Lurie, Rev. Sci. Inst. 33, 1002 (1962)

I. ABSTRACT

15192

Cells that were placed on a 35 - 65 minute automatic cycle of a 50% depth of discharge have reached 4634 cycles. The memory effect was observed, and overcome by two methods.

The theory of oxygen reduction mechanism given in the previous report has been substantiated by other experiments. This theory deals with an H atom mechanism. According to a recent publication, the H atoms are interstitial in the Ni matrix. The theory is consistent with 11 experimental findings. The electrochemical theory is consistent with half of these findings.

Cell efficiency studies were continued. The past work deals essentially with a passivation effect. This effect was studied with controlled potential charging, and related, descriptively, to the constant current charging. Work was also done on the charge efficiency of the positives before the onset of passivation. This was done by the use of porous Ni bodies as the cathodes. Another

II. ELECTRICAL PERFORMANCE OF VO-6HS CELLS

A set of VO-6HS cells that was placed on an automatic 50% depth cycle August 20, 1962, have completed over 4600 cycles. This cycle consists of a 35 minute discharge at 5.15 amperes or 3.0 ampere hours, followed by a 55 minute charge at 3.86 amperes, which corresponds to an 18% overcharge based on the capacity removed. The voltage and temperature of a typical cell are plotted in Figure 1 for cycle number 4634. The temperature shown is the skin temperature of the cell in an environment where convection currents are restricted.

Figure 2 is a plot of end-of-charge and end-of-discharge voltages versus cycle number. These are average values calculated each day from the first cycle of the day. There is a continuous increasing of the end-of-charge voltage and a continuous decrease in the end-of-discharge voltage. Between 3800 and 4000 cycles there was some mechanical difficulty with the relay on the charge circuit, but since this has been fixed, the end-of-discharge voltage has stabilized at slightly above 1.00 volts. It is impossible with this cycle to reduce the end-of-charge voltage without lowering the end-of-discharge voltage too.[1] Because of the "memory effect" these cells have essentially a 3.0 ampere hour capacity and will discharge down to 1.0 volts.[2] Since the period of the charge cycle is fixed, any increase in overcharge must be accomplished by increasing the current, and this will result in high pressures. If the cell is removed from cycle while charged and given a C/10 overcharge for 24 hours the capacity comes back to almost the full capacity.[3] If the cell is discharged to 1.0 volts, then shorted through a one ohm re-

sistor to 0.1 volt, then given a dead short for two hours, followed by a C/10 charge for 24 hours, the full capacity is usually recovered. A second such treatment has always resulted in recovery of the full capacity.

The two experimental VO-6 HS cells which were removed from a 70% depth of discharge cycle due to high pressure were checked for capacity. The capacities were found to be 3.63 and 4.8 ampere hours. After the above mentioned treatment, the capacities were 6.5 and 6.6 ampere hours respectively. After a second treatment followed by a C/10 overcharge for 7 days, the capacities were each 7.6 ampere hours and the overcharge pressures were less than 10 psig.

III. OXYGEN REDUCTION AT THE CADMIUM ELECTRODE

A new theory to explain the reduction of oxygen at the negative electrode was presented in the last quarterly report of this series. Essentially the theory postulated the presence of hydrogen atoms in the grid and matrix of the negative electrode. Oxygen reaches these reaction sites and is reduced.

A number of experimental proofs for this mechanism were discussed. The first set of proofs concerns predictions of a lag in oxygen consumption on a blank cathode when current flow commences, and also a continuing consumption of oxygen after current interruption. These experiments were run and such characteristics were observed.

Since the writing of the last report, another important point was brought to light. If we are dealing with a chemical reaction that causes depolarization, the effect of oxygen pressure on the electrode potential should be small. Another way of stating this, which will be useful, is that while a peroxyl or oxygen electrode should exhibit a slope of 15 mV for a plot of log P vs E, a chemical electrode should exhibit a much larger value of slope. Such measurements were made and large slopes found.[4] In addition, data were taken from Dehmelts and von Dohren's[5] paper, and the slope was calculated. This slope was more in agreement with our data than with the 15 mV required for a peroxyl electrode.

The titanate test for peroxide was applied. The experimental conditions were such as to give large amounts of peroxide if it was formed.

The effect of oxygen on reference electrodes was such as to alter all results from quantitative data into descriptive work. Attempts were made to find suitable reference electrodes. A Hg/HgO, KOH electrode appears suitable for a limited time.

A. REFERENCE ELECTRODES

The nickel oxide electrode when fully charged does show a dependence upon oxygen pressure, which makes a reference electrode of this material suspect. The Cd electrode also shows a potential dependence on oxygen pressure[6,7]. Jany and Ives[8] have reviewed the use of reference electrodes in alkaline solutions, and do not report any suitable under the experimental conditions existing in sealed alkaline batteries. There is the possibility, however, that the Hg/HgO electrode may yield reproducible potentials in so far as oxygen is concerned. Thus, an investigation was started on these reference electrodes.

1. Blank Cell Studies of Pressure-Voltage Relationship

The cells used were described previously. Two sets of data are being reported. One set pertains to a cell having nickel hydroxide anodes and blank cathodes. The other pertains to a cell with silver anodes and blank cathodes. The silver-blank cell was operated at the Ag Ag_2O voltage plateau.

These cells were filled with oxygen and then allowed to stand for at least 15 minutes to ensure no change of oxygen pressure with time. The charge was started which corresponded to a C/10 rate (600 ma) and pressure and voltage were recorded. It is assumed that the anodes could serve

as reference electrodes. It showed that this particular assumption may be invalid, and is the reason for the work on reference electrodes. Another objection to the usefulness of this technique is that polarization may obscure the changes in potential. This may be tested by taking our data even after the pressure in the cell is increasing and hydrogen is being produced.

While hydrogen is being produced, the unimpregnated nickel electrode is expected to behave as a hydrogen electrode. The theoretical slope of log P vs E for a hydrogen electrode is 30 mV.

Examples of data are shown in Figures 3 and 4 for the silver-blank cell and in Figures 5 and 6 for two $Ni(OH)_2$-blank cells the calculated slopes are indicated in the Figures. For the oxygen consumption region these range from 176 to 665 mV compared to a theoretical value of 15mV. In the hydrogen evolution region the slopes range from 20 to 57 mV averaging 38 mV. The average slope is not too different from the theoretical slope of 38 mV. Additional work with more suitable reference electrodes is required to make this work more quantitative.

Dahmelt and von Dohren[5] have performed work which may be subjected to the same analysis. It is given in Figure 5 of this reference. Their data were replotted and is shown in Figure 7. The best slope, as also used with the data in this work, is found to be 233 mV. This value is in sub-

stantial agreement with our lower values of 176 and 186 mV, and again is much different from the theoretical value of 15 mV.

Dehmelt and his co-worker used a $Cd/Cd(OH)_2$ electrode for reference potentials. Because of the effect of oxygen on the potential of this electrode, this work is also descriptive rather than quantitative. The importance of the reference electrode studies is emphasized by the inability to make quantitative observations on the electrodes while they consume oxygen. It should be pointed out that if the reference electrode changes its potential in the same manner as the blank electrodes, the slope will be infinite for the uncorrected measurements. The large values found may be due to this error. The fact that when the electrode evolves hydrogen, it behaves as a hydrogen electrode lightens the burden of suspicion on the silver and $Ni(OH)_2$ electrodes. The question, however, remains unresolved at this time. The value of the method is strongly indicated.

2. <u>The Hg/HgO(C) Pasted Electrodes</u>

a. <u>Experimental Procedure</u>

Six Hg/HgO reference electrodes numbered V-4 - V-9 were prepared as follows:

V-4: Hg - HgO - graphite-water mixture from a mercury cell was pasted on a nickel plated steel grid. The lead consisted of a nickel wire connected to the grid mechanically by twisting. The grid and pasted mixture was then wrapped in a small piece of Pellon V separator

and edge coated with polystyrene in methyl-ethyl ketone for mechanical strength.

V5 and V-6: The edges of a nickel grid were soldered as was the lead wire in each case. The same type mixture was then pasted and pressed on to the grid under a pressure of 15 tons. The edges of the electrode were coated with the same lacquer as V-4.

V-7 and V-8: Silver sinters were used as grids. In the case of V-7, a circular hole was made by scraping off the silver until the X-met showed. In the case of V-8, an entire side of the sinter was scraped off. Silver leads wires were then soldered to each sinter. The sinters were first prepared by amalgamating them in a 0.05 M acidified mercuric chloride solution. Then the sinters were pasted, pressed and lacquered in the same manner as V-5 and V-6.

V-9: Same as V-7, except that a mercury-red mercuric oxide-water mix was used.

The pasted electrodes were immersed in a beaker cell containing 40% aqueous potassium hydroxide. Tank nitrogen (taken as 0 atmospheres O_2), compressed air (0.2 atmosphere O_2) and tank oxygen (one atmosphere O_2) were passed in turn continuously through the electrolyte in the beaker cell. This cell was isolated by a salt bridge from a standard Hg/HgO reference cell in order to prevent the gas purges from affecting the

standard. The changes in potentials of the six test electrodes with time under each purge condition were measured.

b. Experimental Results

All of the electrodes, except V-7 and V-8 were unstable and deteriorated on standing in KOH. Consequently V-7 and V-8 were selected as useful cell reference electrodes. The rate of change of voltage with pressure was found to be 0.0125$\frac{V}{atm.}$ at 1 atmosphere. (See Fig. 8)

B. TIME LAGS

In contrast to the lag P versus E work, the time lag study is difinitive in several respects. First, there is no doubt about the experimental data, and second, it provides a unique differentiation between a chemical and electrochemical mechanism.

The theory which is to be substantiated states that oxygen is reduced by atomic hydrogen in the nickel grid, or on it. A recent paper provides proof of interstitial hydrogen in Ni[9]. If oxygen is added to a cell that contains porous Ni bodies as cathodes, and the hydrogen atoms are removed from the Ni by waiting until the pressure no longer drops, it is reasonable to assume that the Ni is clear of H atoms.

When oxygen is present over clean nickel, and current is passed through to make the nickel cathodic, several cases may occur. If the O_2 is reduced electrochemically, then one expects the pressure decay to be instantaneous with current. Also, when the current is interrupted, the oxygen pressure

should no longer decay. On the other hand, the chemical theory advanced here requires that hydrogen atoms first be put into the nickel, and the oxygen consumption rate is dependent upon the degree to which the atoms are in the nickel. Since the surface is originally clean, then the instantaneous rate should be zero and slowly build up to some steady rate of consumption. A time lag is therefore predicted by the theory.

Continuing this argument, when the current is interrupted there will be some concentration of H atoms in the Ni corresponding to the steady state coverage. It is therefore predicted by this theory that even after current interruption, oxygen will be consumed at a decreasing rate until the Ni is again free of H atoms.

These experiments were run in the blank cells with the oxygen pressure set at 4.4 atmospheres. Such delays were found and are given in Table 3. This technique was not considered sufficiently sensitive since imperceptible movements of the dial could occur instantaneously, and the results may be an error of judgement. A finer experiment was therefore designed.

The refined experiment consisted of reducing the oxygen pressure in the cell to barometric pressure and attaching a 1 ml graduated pipet. The pipet had a drop of water in it to serve as an indicator. The pipet was kept horizontal.

When the current was started, approximately 10 to 20 seconds elapsed before the water column started to move. The

current was interrupted when the water column was near the end of the graduations (0.9 ml). The water column continued to move off scale, and definite motion was perceptible for about 90 seconds after current interruption.

C. PEROXIDE TEST

This test is a very delicate one, and involves the oxidation of Ti^{+4} by hydrogen peroxide, which is thought to yield peroxytitanic acid by some workers. The peroxy-acid imparts a yellow to red color in the presence of peroxide, depending upon the concentration of Ti^{+4}. The test reaction proceeds in acid or even neutral solution. From data given by Wells[10], the sensitivity of the test was calculated to be 0.4 ppm which corresponds to 1.25×10^{-5} M H_2O_2.

Experimental

A 0.03 M titanium sulfate test solution was prepared in 1 M HCl. One drop of this solution, when added to a 0.5% hydrogen peroxide blank in 1M HCl changed the blank from colorless to distinct amber. Then a VO-6 hermetically sealed Ni-Cd cell was pressurized to 50 psig with oxygen and placed on 5A charge for 1 hour. The cell was taken off charge, and within the next 3 minutes, the cell was opened, a negative electrode was stripped from the cell stack and plunged into a solution containing twice the amount of acid needed to neutralize the KOH on the electrode. Within four minutes, 10 ml of titanium sulfate test solution was added.

Results: Under these conditions, peroxide should have been formed and detected, if the necessary reaction with Ti^{+4} occurred. The peroxide test was negative. This test could detect 0.4 ppm H_2O_2. The O_2 consumption is equivalent to 0.001 mole H_2O_2. Upon dilution by neutralization, the concentration of H_2O_2 should be about 0.0007 molar or 3 ppm. Since H_2O_2 is not stable in alkaline solution, the meaning of the negative result can not be interpreted until measurements of the rate of H_2O_2 decomposition are known and compared to the 3 minutes elapsed time between interruption of charge and neutralization.

D. DISCUSSION

For a proposition of oxygen reduction via an electrochemical process, one needs to find the product if it is unique. In this case peroxide, not in the cell normally, is required to substantiate this hypothesis. No peroxide was found within the detection limits of the titanate test.

Secondly, an electrochemical process also requires a Nernst type relationship between the logarithm of oxygen pressure and potential having a slope of 15 mV. While the slope actually found is much different from this value, concurring with Dehmelt and von Dohren's experimental results, it only leads to a suspicion that a depolarization process is occurring by chemical reaction rather than by an electrochemical process. In order to substantiate this suspicion, one needs suitable reference electrodes, the behavior of which in the pressure of oxygen

and hydrogen is known.

The work on the time lags is definitive. Only a chemical process accounts for the slow initial consumption process, and for a continued consumption when current no longer flows through a porous nickel electrode.

There are several key points that the present theory fits that the electrochemical theory does not fit. In addition, no disagreement has been found between the results of investigations by various workers in the field, including the work this laboratory has done, and the theory.

The key points are:

1. While the negative electrode becomes more anodic with an increase of oxygen pressure, the consumption rate does not decrease.
2. The small activation energy of 5 kcal/mole is consistent with a reaction involving atoms.
3. The polarographic curves at Ni does not exhibit an oxygen wave.
4. Peroxide is not found.
5. The consumption lags observed at initiation of current and after cessation of current.

Other points that are fitted equally well by both theories are:

1. Pressure versus current curves are straight lines over wide regions.
2. Anodic shift of potential with increased oxygen pressure.
3. Kinetics zero order in Cd and first order in oxygen.

4. Consumption of oxygen on open circuit by the Cd bielectrode.

5. Decreased oxygen consumption rate in a flooded cell.

6. Faster consumption of oxygen on overcharge than on open circuit.

Thus there are eleven experimental facts, six of which can be equally satisfied by both theories, but the other five are satisfied by the chemical theory given in the previous report.

IV. CHARGE EFFICIENCY

The charge efficiency of a nickel-cadmium cell is dependent upon the efficiencies of the two electrodes. The term "charge efficiency" is ambiguous and requires some clarification. This clarification arises from the experimental results contained in this and the previous quarterly report.

When a cell is being charged at a current I, some of this current is producing a side reaction. For example, while $Ni(OH)_2$ is converted to NiOOH some oxygen is being formed by the oxidation of OH^-. This, then provides one definition of a charge efficiency.

At some later time, measured as charge input, there is a change of charge efficiency to a fairly low value. This is exemplified by the Cd electrode. This electrode exhibits a step change in potential to a more cathodic voltage and simultaneously evolve gaseous hydrogen. For the purposes of this discussion, it is the change of dominant electrode process that is more important than the potential change. This change of dominant process is termed passivation.

There is another term in common usage related to charge efficiency. This term is the utilization coefficient. It is defined as the ratio of discharge capacity to the theoretical capacity. It is a quite useful term, but it is confounded by the discharge rate and the charge efficiency in the two senses given above.

During the past quarter, additional work was done on the charge efficiency as governed by passivation of the electrodes. Work was instituted on the charge efficiency concerned with side reactions.

which, for convenience is termed the current efficiency.

The current efficiencies of the nickel oxide electrodes were measured by means of special cells which contained positive electrodes and unimpregnated negatives. For a given current a theoretical oxygen consumption rate can be calculated. Deviations of the experimental values from the theoretical values indicate the amount of current going into a side reaction.

There are two possible side reactions. One is the electrochemical oxidation of hydroxyl ions to oxygen and water, and the other is the formation of unstable oxides of Ni^{11}. The unstable oxides can be measured by open circuit pressure changes immediately after charge. There is a complication, however, since cells will be used and oxygen is consumed by the negative electrodes. A theoretical analysis is presented which allows interpretation of the data.

A. PRESSURE CHANGES AT THE END OF CHARGE

In the two previous quarterly reports in the work on the charge efficiency of the nickel oxide-cadmium alkaline system several curves were shown which were indeed interesting. These are the curves of the pressure changes in a cell after charging and evacuation.

The typical aspects of these curves were that the pressures at first increased rapidly, then they leveled off and finally started to decrease. These curves are to be expected on the basis of the self-discharge processes that the positive electrodes exhibit, and the oxygen reduction process that occurs at the negative electrode.

Such experimental data can, at least in principle, afford information on the overcharge process and charge efficiency of

the positive electrode. This is one of the objectives in the contract. In addition, information can be gained on the self-discharge processes. This can be used as an adjunct to some information already available on these processes. A third area of information will be on the oxygen reduction process. This last process is also part of the objectives of the present work, and separate experiments are reported in another section of this report.

In order to obtain maximum information from these data, (it is necessary to eliminate the effects of the second consecutive self-discharge process and the oxygen consumption process) a method is needed. This method is supplied by a theoretical consideration of the system we are studying. The law that describes the self-discharge is known as is the law that describes oxygen reduction. By using these laws in differential form to explain the pressure behavior and solving for the initial rates, the derived function is the method used for analyzing the experimental data. This treatment is given in detail in the next section.

1. Theory

The oxygen evolution processes from charged nickel oxide electrodes have been shown to consist of an oxygen source which yields oxygen in two consecutive processes. The first process has a rate constant approximately 10^{-2} per minute while the second is approximately 1/20 of this rate[11]. There is some evidence for a third self-discharge process in which oxygen is evolved, and, if it is also a

first order reaction, its decay constant is estimated to be about 10^{-4} per minute[12]. Another oxygen evolution process takes place, but it is zero order and extremely slow. It shall be neglected in this treatment.

The oxygen reduction process is independent of the state of charge of the negative electrode, at least above about 2/3 atmosphere partial pressure of oxygen. Above this pressure the reaction is first order with respect to oxygen. Below 2/3 atmosphere oxygen is still reduced, but the specific velocity constant is considerably less than for the higher pressure condition. In addition, when a cell is completely flooded so that all the active material is below the electrolyte level, oxygen is still reduced. The rate constant for flooded cells is smaller than for unflooded cells*.

In order to set up the differential equations which govern the behavior of charged-evacuated cells, several assumptions will be made, for clarity and simplicity, which probably do not significantly affect the conclusions. First we shall assume that only the first two rapid self-discharge reactions of the positive nickel oxide electrode are significant. Second, we shall assume that the transition from the high pressure oxygen reduction reaction to the low pressure reaction is discontinuous. In this manner, we do not need the function relating the rate constant to the pressure, but merely substitute the appropriate value depending upon the pressure range encountered in the ex-

*The rate constant is that of a heterageneous reaction so that changes may be effective changes corresponding to different surface areas or reaction sites.

periments. It is therefore, to be recognized that this sort of treatment is a first approximation having a validity governed by the validity of the assumptions.

For the electrodes involved in these experiments the normalized oxygen evolution rate is,

$$(1) \qquad \gamma = \frac{A^o}{C} \left\{ (1 - e^{-k_1 t}) + (1 - e^{-k_2 t}) \right\}$$

where A^o = amount of oxygen source material at the instant of current interruption,

C = capacity of the positive electrode expressed in the same units as A^o,

k_1, k_2 the rate constants for the two oxygen evolution processes, units of reciprocal time

t = time

By multiplying equation with a factor, α, it can be given in terms of pressure. This equation is needed in the form of the derivative which is the increase of pressure due to the self-discharge reactions at the positive electrode,

$$(2) \qquad \left.\frac{dP}{dt}\right|_{rise} = \frac{A^o \alpha}{C} \qquad k_1 e^{-k_1 t} + k_2 e^{-k_2 t}$$

The oxygen reduction reaction, under the assumption made, is given simply by,

$$(3) \qquad \left.\frac{dP}{dt}\right|_{decay} = -k_g t$$

where k_g is the rate constant for oxygen reduction from the gas phase.

The net pressure change in a cell after interruption of charge, provided it is in overcharge for a sufficiently long period, is:

$$(4)\quad \left.\frac{dP}{dt}\right|_{net} = \frac{\alpha A^{o}}{C}\quad k_1\exp(-k_1 t) + k_2\exp(-k_2 t)\quad -k_g P.$$

When both sides of the equation are multiplied by $\exp(k_g t)dt$, the equation may be integrated. Instead of assuming that the cell is evacuated at charge interruption, we shall merely state that at $t = 0$ the pressure of oxygen within the cell is P_o. Using these boundary conditions, the final form of the equation is,

$$(5)\quad P = \frac{k_1\ A^{o}}{C(k_1-k_g)}\left\{(1-e^{-k_1 t}) - (1-e^{-k_g t})\right\} + \frac{k_2\ A^{o}}{C(k_2-k_g)}$$
$$+ \frac{k_2\ A^{o}}{C(k_2-k_g)}\left\{(1-e^{-k_2 t}) - (1-e^{-k_g t})\right\} + P_o e^{-k_g t}.$$

I If equation 5 is differentiated and set equal to zero, it can be seen that the time to reach a maximum pressure will be dependent upon the initial pressure. Another useful expression may be derived from equation 5. To determine the initial pressure change rates the exponents may be expanded and the squared and higher terms neglected yielding,

$$(6)\quad \lim_{t\to o}\frac{P}{} = \frac{k_1\ A^{o}}{C(k_1-k_g)}\left\{k_1 t - k_g t\right\} + \frac{k_2\ A^{o}}{C(k_2-k_g)}\left\{k_2 t - k_g t\right\} + P_o(1-k_g t).$$

Equation (6) may now be differentiated to yield,

$$(7)\quad \text{Rate}_{initial} = \frac{\alpha A^{o}}{C}\quad (k_1 + k_2) - P_o\ k_g.$$

Consider equation (5). If the positive electrodes are isolated, kg may be set equal to zero since oxygen reduction can not occur. The resulting equation is then idential with

equation 1, as it should be. Also, as P_o is increased in magnitude, the effect of the other terms on the right hand side is diminished. That is to say, that the maximum pressure rise is decreased as P_o is increased. It also follows that the time to reach a maximum pressure is decreased as P_o is increased. At high enough values of P_o, the time to reach the maximum pressure will be zero.

Equation (7) indicates that the pressure due to oxygen within a cell is decreased continuously, and it will affect the initial pressure changes. As a matter of fact, when the second term on the right hand side is greater than the first term, there will be only a decrease in pressure.

Fitting of equation (7) to the data obtained in the last quarterly report and during the quarter covered by this report will constitute the remainder of this section. The values of each constant term will be ascertained. By assuming that all the k's remain unchanged, the effect of overcharge current on A^o will be determined. Then by varying temperature the effect upon initial rates will be determined. The value of k_g can be changed by flooding the cells.

2. Experimental

Several nickel-cadmium prototype cells were used. A diagram of one was shown in Figure 6 of the Eighth Quarterly Report. The diagram depicts a pressure transducer. Nine of the cells used had a bourdon tube pressure gauge, and one cell was equipped with the transducer. A constant current supply[13] was employed across the potentiometer of the transducer. The output was recorded on a Bristol Single Pen re-

corder scanning at 4 inches per hour. The full scale of the recorder corresponded to 2 atmospheres.

Cells were charged at a constant current obtained by ballasting a 30 volt DC line supplied by a constant potential source (a Vickers Welding supply). When each cell was in overcharge the pressure was adjusted to the desired level. This was accomplished by evacuation and/or pressurization with oxygen. When the pressure was brought to the appropriate point the cell was sealed and the current simultaneously interrupted. This technique was employed not only during the quarter just completed, but during the prior quarter. The data taken and recorded in the Eighth Quarterly have a lapse in time between charge interruption and evacuation, and can not be used in a quantitative manner.

3. Results

a. Oxygen Decay Curves

In order to obtain an order of magnitude for k_g under various conditions, oxygen pressure decay curves were determined on a cell when in an unflooded condition, and also later when flooded. These data are shown in Figure 9. The effective rate constant for an unflooded cell is approximately 50 times greater than for a flooded cell in the higher pressure region above 2/3 atmospheres.

b. Unflooded Cells

The pressure changes encountered in sealed cells are expected to follow equation 5. The cell was charged

at C/10 for 24 hours at 77°F (oil bath). The pressure adjusted at zero for the first run and 1/3 atmosphere higher on each run thereafter until the initial pressure, P_o, was 1-1/3 atmospheres. The pressure gauge, a bourdon tube, was read visually. A plot of the pressure versus time is shown in Figure 10. The initial rates, at which the pressures rise, decrease with an increase in P_o. The maximum pressure rise also decreases with P_o until, with the cell tested, at 1-1/3 atmospheres there is no perceptible rise at all. The pressure decay after the maximum is reached appears to increase with increasing P_o, and the time to reach the maximum appears to steadily decrease with an increase in P_o.

The initial pressure rise as a function of P_o is shown in Figure 11. The equation that fits the straight line shown in this Figure is:

(8) $R_{init} = 0.070 - 0.053\ P_o$.

Equation (8) has the same form as (7).

The time for the pressure to reach a maximum value is plotted versus the initial pressure in Figure 12, and the maximum pressure rise is plotted against the initial pressure in Figure 13.

The data of the last quarterly report for initial pressure rise at several low temperatures are plotted versus the charge rate in Figure 14. Three charge rates were used. Since a cell that is not charged at all can not have a pressure rise, these data were extrapolated to the origin. These data will satisfy equation (7)

when P_o is set equal to zero. Since the initial pressure rise at each temperature is dependent upon the charge rate, A^o must be dependent upon the charge rate. The slope of each line is therefore given by $(c/\alpha)(k_1+k_2)$. But $k_1 \sim 20\ k_2$, and the activation energy of the rate constant k_1 may be obtained by taking the slope of a plot of the relative slopes of Figure 7 against the reciprocal of absolute temperature. This is shown in Figure 15. This slope corresponds to an activation energy of 3.92 kcal/mole.

c. Flooded Cells

Since the oxygen consumption rate is decreased by an order of magnitude or more when a cell is flooded, equation (7) becomes simplified. The last term may be neglected while taking the initial rate data.

Cells were flooded until the electrolyte was above the level of the plates. The pressure transducer was used to record the changes. The results obtained at a 0.6A charge rate at 77^oF are given in Table I. It is seen that the initial pressure increase rate is essentially independent of the initial oxygen pressure. The total amount of rise is also virtually independent of the initial pressure. These are the results to be expected for flooded cells on the basis of the theory developed.

An example of the strip chart record is shown in Figure 16. It is seen that after a sufficiently long

time the pressure does decay. This is to be expected when the elapsed time is long enough to invalidate the necessary assumption for initial rate data.

It is possible to have flooded sealed cells accept an overcharge. This is achieved by continued venting of the cells when the pressures reach about 100 PSIG. When such cells are in overcharge, apparently nearly all oxygen transfer is from the positive electrode in a dissolved form. If this is true, then no pressure rise is expected. Figure 17 shows that this, indeed, is what occurs.

B. BLANK ELECTRODE CELLS

The blank electrode cells were described earlier. They are identical with the previously described cells, but the negatives are unimpregnated. These cells are pressured with oxygen and then placed on charge. Oxygen will then be consumed during charge. If the oxygen consumption rate is less than theoretical, the difference is ascribed to oxygen generation at the positives which decreases the current efficiency of the system.

The results reported here are preliminary in nature. Internal checks on the method were obtained using a silver anode in place of the Ni $(OH)_2$ anode. These cells were constructed primarily for an investigation of the oxygen reduction reaction. Several were constructed with reference electrode. These data are presented elsewhere in this report.

1. Theory

When current is passed through a Ni $(OH)_2$ - blank or Ag-blank cell there are electrochemical processes occurr-

ing at both electrodes. For the Ni $(OH)_2$ electrode we postulate the following:

(9) $Ni(OH)_2 + OH^- \xrightarrow{i} NiOOH + H_2O + e^-$

(10) $4\ OH^- \xrightarrow{i} O_2 + H_2O + 4e^-$

(11) $Ni(OH)_2 + OH^- \xrightarrow{i} A_1 + e^-$.

Equation (9) is the conversion of the discharged material into active material. Equation (10) represents the possibility of the direct evolution of oxygen by an electrochemical process. Equation (11) is the electrochemical formation of the unstable oxygen source[11]. This source decays into a second source, A_2, with the simultaneous evolution of oxygen. A_2 decays again releasing additional oxygen. These decompositions may entirely account for the oxygen found, eliminating the necessity of postulating the oxidation of hydroxyl ion given in equation (10). Regardless of the particular mechanism, any current going into the reactions 10 or 11 will be evidenced as oxygen. It is this fact that makes the method of study used here a feasible method.

At the silver anode, the following reactions occur sequentially:

(12) $2\ Ag + 2OH^- \xrightarrow{i} Ag_2O + H_2O + 2e^-$

(13) $Ag_2O + 2OH^- \xrightarrow{i} 2AgO + H_2O + 2e^-$.

Equation 10 is postulated as a possible side reaction, especially during charge at the upper plateau corresponding to equation (13). The potential will determine the processes occurring. Equation (12) occurs at a potential

less anodic than equation (9), but equation (13) requires a more anodic potential than equation (9) increasing the likelihood of the oxidation of hydroxyl ion. Of course, this must be tempered by the overvoltage of oxygen upon the electrode involved.

Consider the experimental cell. It has a gas volume V, is charged at I amperes at an absolute temperature T, and is pressured with oxygen to P atmospheres. When the oxygen is consumed at the negative blank electrode, it must do so at a rate proportional to the current. Using the ideal gas law, we may write the pressure decay as:

$$(14)\quad \frac{dP}{dt} = \frac{RT}{V}\frac{dn}{dt} ,$$

where n is the number of moles of oxygen consumed and the other symbols have their usual significance. Multiplying by the number of electrons required to produce a molecule of oxygen, 4 N, and using the relationship (N = Avogadro's number)

$$(15)\quad I = zF\frac{dn}{dt} ,$$

where F is the faraday of electricity,

$$(16)\quad \frac{dP}{dt} = \frac{RT}{4FV} I .$$

Equation (16) therefore represents the theoretical rate of oxygen consumption, and is expected to hold until the oxygen pressure decreases to the point where this process no longer occurs. At this time it is expected that the potential will increase as the blank electrode changes from an oxygen con-

sumption electrode into a hydrogen evolution electrode.

The pressure rise during hydrogen evolution should occur at approximately twice the rate at which oxygen is consumed, since only 2N electrons are required to produce a mole of hydrogen.

2. Results

Several cells were prepared for this work. The volumes were determined by a gas expansion procedure. A cell case and cover with a pressure gauge were used to form a pressure vessel. Its volume was determined with water. It was pressured with N_2 (He gave the same results), connected to the evacuated cell, the volume of which was being determined. From the pressure drop, the volume of the cell was determined.

The cells were evacuated, then pressured with oxygen to approximately 50 PSIG. During a 0.6 A charge, the pressure decay rates were measured manually, and data taken corresponding to oxygen consumption, and finally into the region of hydrogen evolution. The terminal voltage was simultaneously measured.

Typical data for a nickel-blank cell are shown in Figure 18, and for a silver-blank cell are shown in Figure 19. During the oxygen consumption period the cell voltage is fairly stable, even at the lower pressure region. The sharp rise in voltage occurs in the neighborhood of the hydrogen evolution region. The flattening of the curve at the higher oxygen pressures is not

unexpected. The Nernst equation for a hydrogen electrode leads one to expect the voltage to be proportional to the logarithm of hydrogen pressure, which accounts for the relatively low rate of change of terminal voltage with increasing pressure.

The pressure behavior is, in most respects, that which was predicted in the theoretical section. Oxygen is consumed at a rate approximately related to current. Hydrogen is evolved later at approximately twice the rate for oxygen consumption.

The first cell investigated in this manner was initially used for other experiments, and it turned out that the positives were nearly fully charged. The charge efficiency is given in terms of the deviation of the slope from the theoretical slope. It averaged 27% low.

A cell using silver anodes and blank cathodes was next investigated in both the oxygen consumption and hydrogen evolution region. These results are given in Table II. A second nickel oxide-blank cell was made. In this case the electrodes were discharged initially so that changes in efficiency could be determined as a function of the state of charge. These data are also in Table II.

These data are considered preliminary in nature. The errors in measuring volume and current is small enough to be ignored. The pressure measurements from which the rate determinations are made is estimated to be about 3%. Another source of error is in the use of the ideal gas law,

and may also be a few percent.

The rate determination errors should be random. The use of the ideal gas law will yield results that are low, so that the net result is that Table II would have negative signs indicating negative deviations.

As a first approximation we may neglect the errors, and give the charge efficiency of the positive electrodes as shown in Figure 20. These 3 points, represent the average values of oxygen consumption deviation from theoretical in the intervals indicated by the horizontal arrows. These are for VO-6 HS type positive electrodes charged at 75°F at C/10. These points do indicate that the current efficiency of the positive electrodes is always less than unity and is dependent upon the state of charge. The decreasing efficiency indicates further the need for overcharge in order to completely convert the $Ni(OH)_2$ into the higher oxide.

C. UTILIZATION OF ACTIVE MATERIAL

1. Experimental Procedures

Eight 6 ampere hour hermetically sealed cells were employed in groups of four cells to complete the controlled potential charge efficiency tests at temperatures of 50, 25, 0 and -15°F. Each group of four cells were first brought to one of the selected temperatures; then one cell of a group was charged at one of the test potentials which were 1.45, 1.50, 1.55 and 1.60 volts. The charging procedure and circuit employed has been described in detail in

the Ninth Report. The pressure changes during each charge were monitored at frequent time intervals. The ampere-hour input at any time during the charge was determined by integration of the current-time curve obtained by means of a single pen recorder model. The type of gas evolved was again determined by ignition.

After completion of charge, each cell was discharged at 3A to 1.0 volt.

2. Experimental Results

The curves relating pressure changes during charge to charge input at the experimental temperatures and potentials are given in Figures 21 - 24. It may be seen that the charge input required to produce gas decreases as the charge potential is increased, while the input increases as the temperature is decreased from 50° to 25°F (Figures 21 and 22). However, at the 0° temperature (Figure 23), the order of gas initiation is reversed with regard to charge input, that is, charge input for gas onset decreases as charge potential is decreased. At -15°F (Figure 24) the order is again reversed and is the same as is given for the 50° and 25° temperatures. Thus two inversion points were obtained which may be again implied from an examination of Figure 5, where charge potential is plotted versus charge input to start pressure rise. The inversions are indicated clearly by the near-asymmetry of the 0° to 50°F isotherms and the displacement of the -15° isotherm, which is out of sequence. There appears

to be an inversion charge potential in the vicinity of 1.553 volts. In Figure 26, where temperature is shown as a function of charge input for gas production, the graph is more informative than Figure 25. The equipotential contours intersect in two points, corresponding to two inversions in the sequence of charge input. The inversion temperatures are at approximately +10 and -10°F. It should also be noted that the gases evolved (shown at the dotted line isotherms in Figure 26) was oxygen at 50 and 0°F and hydrogen at 25°F and -15°F.

Steady state pressures and/or pressure rise to 150 PSIG were obtained throughout the tests. Figures 21 - 24 show that the magnitudes of the developed cell pressures increase with increasing charge potential and temperature. This applies to steady state cases as well as those in which 150 PSIG was reached during charge.

The capacities of the cells upon discharge at 3.0 amps to 1.0 volt are given in Table III.

D. DISCUSSION

The theory developed to help interpret the pressure change data obtained after charge did yield mathematical expressions that are in agreement with experiment. From application of this theory it is deduced from Figure 14 that the amount of the first unstable nickel oxide formed is dependent directly upon the charge current and is also dependent upon temperature.

The blank cell work shows that there is a side reaction that is responsible for a current efficiency of less than unity. The efficiency does appear to be dependent upon the state of charge of the positive electrodes as seen in Figure 20. This indicates the need for an overcharge in the nickel-cadmium system in order to obtain full capacity.

It has been previously reported [14] that at low charge rates the capacity of Ni-Cd cells is decreased. A plot of these data is shown in Figure 27. If this fall-off of capacity at the lower charge rates is due to formation of unstable oxides, then one would expect that the amounts formed at lower charge rates would not decrease. Experimentally they do decrease. It is therefore presumed that the parasitic reaction responsible for the lessened capacity at low charge rates is due to the generation of oxygen as given in equation (10). If the negative deviations given in Table I for the silver electrode is real, instead of containing an error of comparable magnitude due to use of the ideal gas law, then one would presume that equation (10) also occurs in this system. Generally, the charge efficiency of the silver-cadmium system is high, 96 to 98%. The agreement between the results of this work and the results of others on the charge efficiency tends to provide additional support for the conclusion that hydroxyl ion converted electrochemically to oxygen and water is the side reaction responsible for the lowered charge efficiency of the positive electrodes.

The controlled potential charge method is considerably more complex in analysis than the constant current method. However, if the controlled potential charge curves are characterized by their component parts, the factors affecting cell behavior under controlled potential charge conditions will be uncovered.

In Figure 28 is shown a typical set of controlled potential charge curves obtainable at any temperature under the experimental conditions. It will be seen that any of the controlled potential charge curves are separable into three parts: (1) a limiting current region, which is in reality a constant current charge; (2) a current decay portion; and (3) a plateau region, which may be regarded as a second constant current charge. These curves should be in many respects similar to a step-type charge, and indeed this is supported by the data. It was found during the course of the tests that each portion of a given curve varied with charge potential and temperature in a specific manner independent of the remainder of the curve, but in a definite relation to other curves in the group(s). Thus, it was found that region 1 in this figure increased in length as the potential and temperature increased; the slope of region 2 increased in magnitude with increasing potential and temperature; the current associated with regions (1) and (3) increased with increasing potential and temperature.

In previous work with constant current charging, it was found that the efficiency of the positive is enhanced as the

current is increased, while the efficiency of the negative is increased as the current is decreased. The side reaction associated with efficiencies $<$ unity are the oxidation of water at the anode to form oxygen and the reduction of water at the cathode to form hydrogen. Furthermore, the negative is depolarized by oxygen reacting with adsorbed hydrogen on it to form water. It was also indicated that the relative efficiencies of the electrodes determine cell behavior during charge. With these factors at hand, the controlled potential curves will now be treated in terms of electrode efficiencies.

An examination of Figure 28 shows that there are three distinct types of curves to be studied:

Case I. The limiting current is of sufficient duration to fully charge the positive. Under these circumstances the positive has an efficiency near unity, because we are going into overcharge at constant current. Furthermore, shortly after region 1, the current decays rapidly, and the positive is becoming relatively less efficient than the negative, especially at the low plateau current. Consequently, after oxygen is consumed for depolarization of the negative, excess oxygen will be evolved to 150 PSIG or steady state pressure will be achieved. (See Fig. 21)

Case II. The limiting current is not of sufficient duration to fully charge the positive.

There are two possibilities here: (a) full charge of the positive may be attained at some point on the de-

cay portion (region 2) or (b) not. If the former is the case, then the positive becomes inefficient later than in Case I, while the negative is relatively inefficient for a longer period of time at this high current. Thus hydrogen will be evolved at 150 PSIG or steady state (see Figure 22). If (b) is the case, the current will decay rapidly, at some point the negative will be effectively depolarized, the current will fall to a low level to enhance negative efficiency, and oxygen will be evolved (see Figure 23).

Case III. The limiting current is so low and the length of the decay portion so long that the negative is again relatively less efficient than the positive so that hydrogen is evolved. This is clearly the case depicted by Figure 24. Also, depolarization of the negative occurs very sluggishly at this low temperature, since the reaction to form water is not electrochemical.

In regard to Figures 21 - 24 cited above, it should be noted that each case given was meant to explain the behavior of individual curves within a group and not the whole group. Probably all cases may occur within a group. But, the explanations given above were designed to indicate the many ways that the factors involved could combine and influence electrode efficiency and lead to the inversions shown in Figure 26.

Although the cells had varying charge inputs, the discharge data given in Table III are useful, since in most instances, the cells were allowed to reach 25% or better overcharge which is sufficient, as indicated in previous reports, to establish cell capacity. It can be seen immediately that cell capacity increases as the charge potential increases, and decreases as the temperature decreases. These data, along with the results obtainable from Figures 21 - 24, indicate that the optimum charge potential and temperature consistent with the criteria of low pressure, reasonable duration of charge and safe overcharge currents, would be 1.50 volts at 25°F. This selection would yield 7.0 AH out, for 9.3 AH in, with a developed pressure of 23 PSIA.

V. IMPROVED ELECTRODES

Research and development efforts on nickel-cadmium cell electrodes were aimed at improving the energy to weight and energy to volume ratios, with the primary emphasis placed on the former. It was felt that an increase in the ampere-hour capacity of an electrode of a fixed size and weight, would result not only in a better weight efficiency, but an improved volume efficiency as well. Our approach was such that an improvement in one area meant an improvement in the other one also.

The Gulton VO-HS series cells which have been designed specifically for space applications are such that about 55% to 60% of the total cell weight represents the weight of the positive and negative plates. Consequently, about 0.061 to 0.066 ampere-hours/gm of plate are required to achieve a 20 watt-hour per pound ratio for a cell (0.061 AH/gm are required for the VO-20 HS cell and 0.066 AH/gm are required for the VO-6HS cell to achieve the 20 watt-hours per pound). For these reasons results will be discussed in terms of weight gain or AH capacity achieved per unit weight of plate.

Development efforts to achieve higher plate loading have been concentrated on techniques to effectively load more dissolved nickel and cadmium into the sintered carbonyl nickel plaques. Nickel nitrate and cadmium nitrate were dissolved in low surface tension solvents in such concentration that one cc of solution contained one gram of the salt. The plate was immersed in the solution, dried, and the nitrate converted to the corresponding hydroxide by treatment with KOH. The plate was then washed to remove excess KOH and dried. This cycle was repeated until the desired pickup was achieved. The impregnated plates were then assembled into vented, flooded cells and charge-discharge cycled at the two hour rate to determine the AH capacity.

In the early phases of this program impregnation of plates using molten salts were also examined. $Cd(NO_3)_3 \cdot 4H_2O$ (m.p. 59.4°C) and $Ni(NO_3)_2 \cdot 6H_2O$ (m.p. 56.7°C) were heated to 80°C and used in the impregnation cycle described above. However, after two trials, the results achieved by this technique were so poor compared to the low surface tension solvent method that this approach was abandoned.

If the active materials are used with a 100% efficiency 3.46 gms of $Ni(OH)_2$ and 2.72 gms of $Cd(OH)_2$ (the active material while the cell is in the discharge state) are required for one AH of capacity. Earlier work had shown that while the positive active material can be utilized with a 100% efficiency, the negative one is only 80% efficient. This means that 3.40 gms of $Cd(OH)_2$ are required for one AH of capacity. In addition, for successful sealed cell operation, an excess negative capacity is desirable. Assuming that a 30% excess negative capacity is required for overcharge capability, the amount of $Cd(OH)_2$ needed for one AH is increased to 4.42 gms. That brings the total amount of active material required to 7.88 grams /AH for a sealed cell.

Results of active material impregnation using low surface tension solvents, are summarized in Figures 29 to 31.

Figure 29 shows the positive active material pickup as a function cycles. As may be seen, the pickup is uniform for the first three cycles, but as the plate becomes loaded, the pickup diminishes. As the figure indicates, a continuation of the impregnation cycling would in all probability result in an even greater pickup. However, our aim has been to achieve a certain plate loading, and after this goal had been achieved, the process was stopped.

Figure 30 shows the active material pickup for negative plates. As may be seen, a much higher loading is possible for an equivalent negative plate. In fact, four to five cycles would have been sufficient to match the desired capacity based on the available positive capacity. Any excess negative capacity beyond that which is required merely serves to reduce the watt-hour per pound ratio of the cell.

Figure 31 shows the actual AH capacity achieved when the cells were cycled at the two hour rate. Values are based on the weight of both positive and negative plates, assuming that the weight distribution between positive and negative plates are divided in a ratio of 45 to 55. As may be seen, we have achieved a figure of 0.0658 AH/gm of plate, or 20 watt-hours per pound of cell when discharged at the two hour rate to 1.0 volt per cell.

VI. CONCLUSION

This report is the last of a series of Quarterly Reports under Contract NAS 5-809. These 10 reports contain the results of experimental work to design, develop and manufacture storage batteries for satellites. The last 3 reports of the series include, in addition, work on electrode improvements, charge efficiency and a fundamental investigation into the reduction of oxygen at the negative electrode of the sealed sintered plated nickel-cadmium system.

The highlights of the work performed will be reviewed and presented in a Final Report. This report will summarize the advances and findings of the ten quarters during which the contract ran.

Some significant advances have been made under this contract and Gulton Industries expresses their appreciation to NASA for their support.

VII. PERSONNEL

The following staff personnel worked on this project during the past quarter:

Dr. R. C. Shair	Director of Research
Dr. H. N. Seiger	Asst. Director of Research
E. Kantner	Senior Chemist
A. Lyall	Chemical Engineer
H. Cohen	Physical Chemist

TABLE I.

PRESSURE RISE AS A FUNCTION OF INITIAL OXYGEN PRESSURE CHARGE AT 0.6A FLOODED CELL 77°F

INITIAL PRESSURE atm.	INITIAL RATE OF PRESSURE RISE atm/min.	MAXIMUM PRESSURE RISE atm
0.01	0.032	0.41
0.20	0.034	0.43
0.40	0.035	0.41
0.59	0.029	0.31
0.78	0.034	0.39
0.94	0.040	0.44
Average	0.036	0.40

TABLE II.

DEVIATION OF OXYGEN CONSUMPTION AND HYDROGEN EVOLUTION RATES FROM THEORETICAL VALUES (BLANK CELL DATA).

CELL	EXP. NO.	DEVIATION OF O_2 CONSUMPTION, %	DEVIATION OF H_2 EVOLUTION, %
Ni Blank (1)	3/12 -1	-28	-32
Ni Blank (1)	3/13 -2	-24	-24
Ag Blank	3/13 -1	-4	-12
Ag Blank	3/14 -2	-3	-8
Ni Blank (2)	3/15 -1	-7	-4
Ni Blank (2)	3/15 -2	-14	-4
Ni Blank (2)	3/15 -3	-18	-23

TABLE III.

CAPACITIES OF CELLS CHARGED AT CONSTANT POTENTIALS

DISCHARGES AT 3A TO 1.0 VOLT
* Capacities in Ampere-Hours

CHARGE POTENTIAL volts	50°F	25°F	0°F	-15°F
1.45	6.2 (8.3)	5.9 (8.4)	5.2 (5.5)	3.0 (4.6)
1.50	6.8 (13.6)	7.0 (9.4)	6.8 (10.2)	5.8 (7.6)
1.55	7.0 (14.3)	7.2 (9.3)	7.1 (11.7)	5.7 (8.6)
1.60	7.4 (11.1)	7.8 (14.8)	6.7 (14.3)	6.9 (11.5)

* Charge inputs are in parenthesis

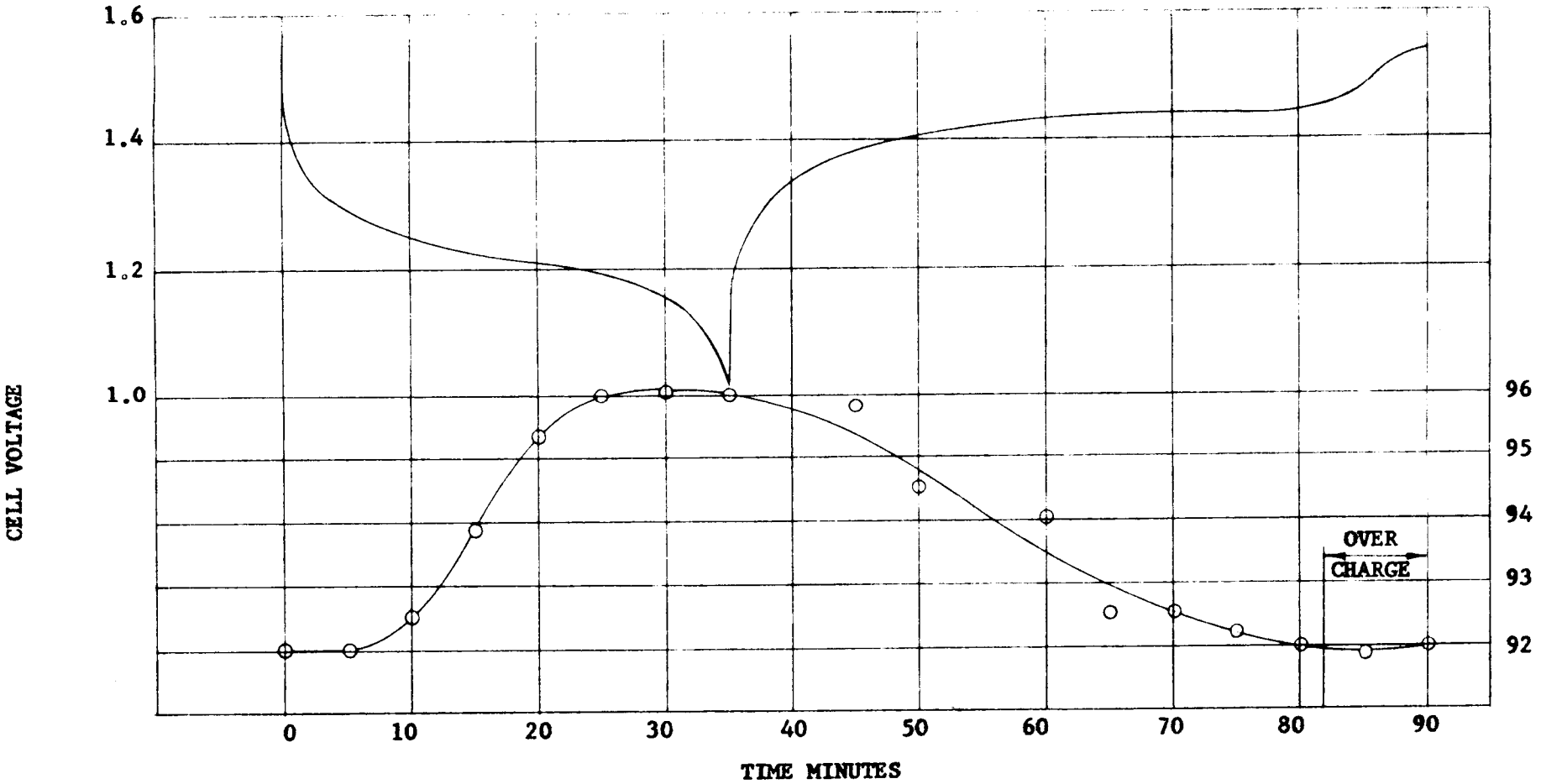

M1676
AB3000-10

Figure 1 Cycling of VO-6 HS Cells: Cycle No. 4634, 50% Depth

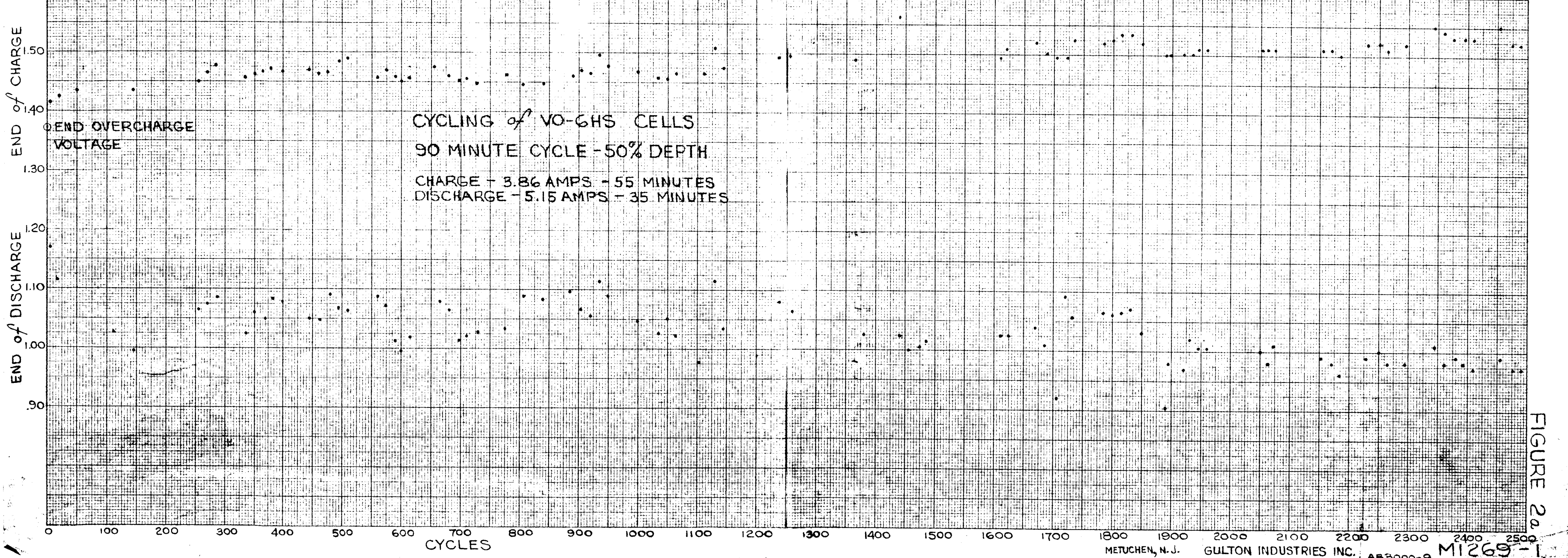

FIGURE 2a

M1269-1

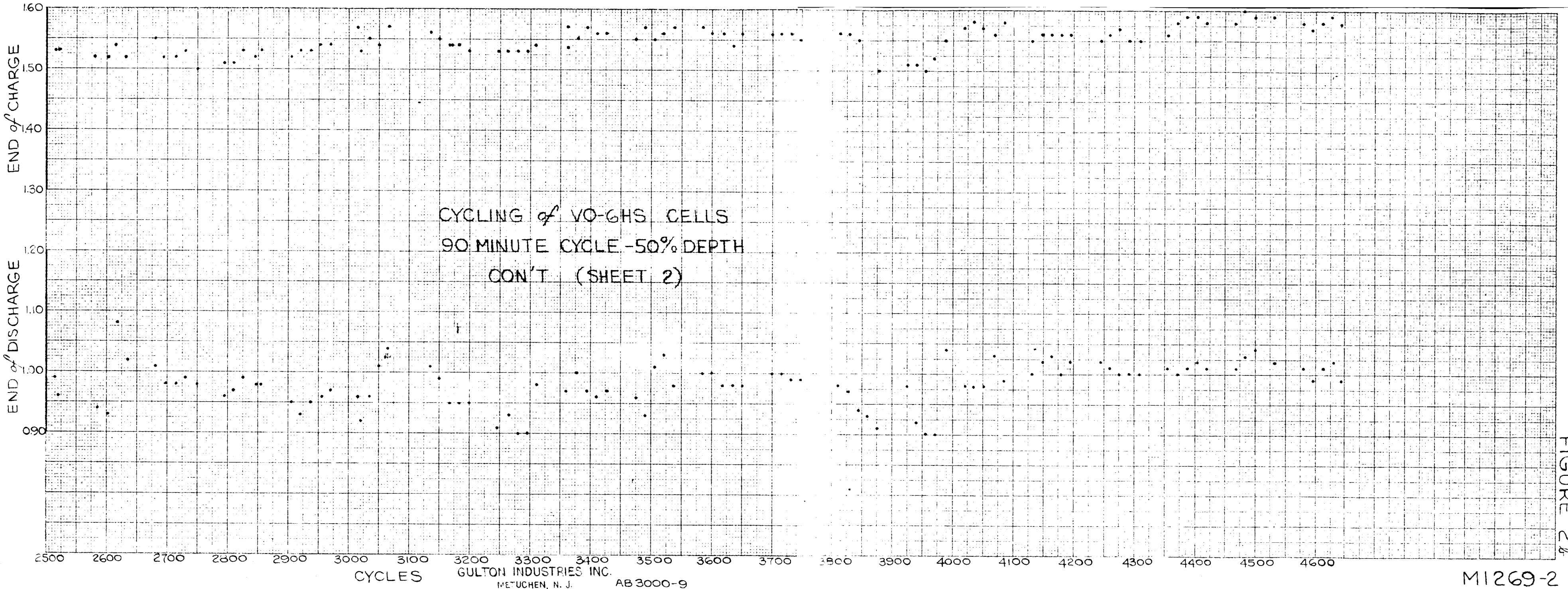

FIGURE 24

M1269-2

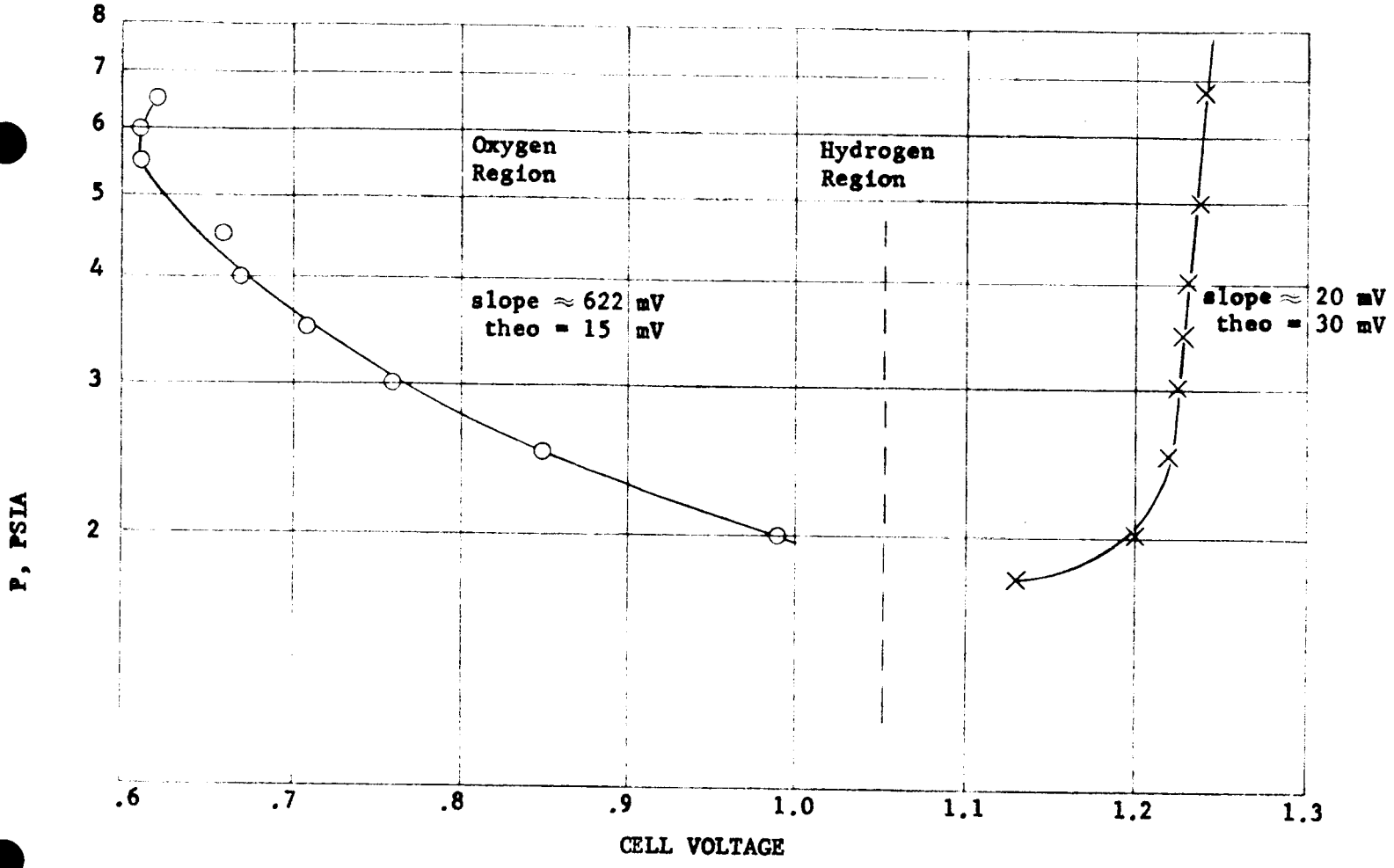

Figure 3 Pressure - Voltage Curves During Oxygen Consumption and Hydrogen Evolution in a Silver-Blank Cell at C/10 Charge Rate - Run No. 1

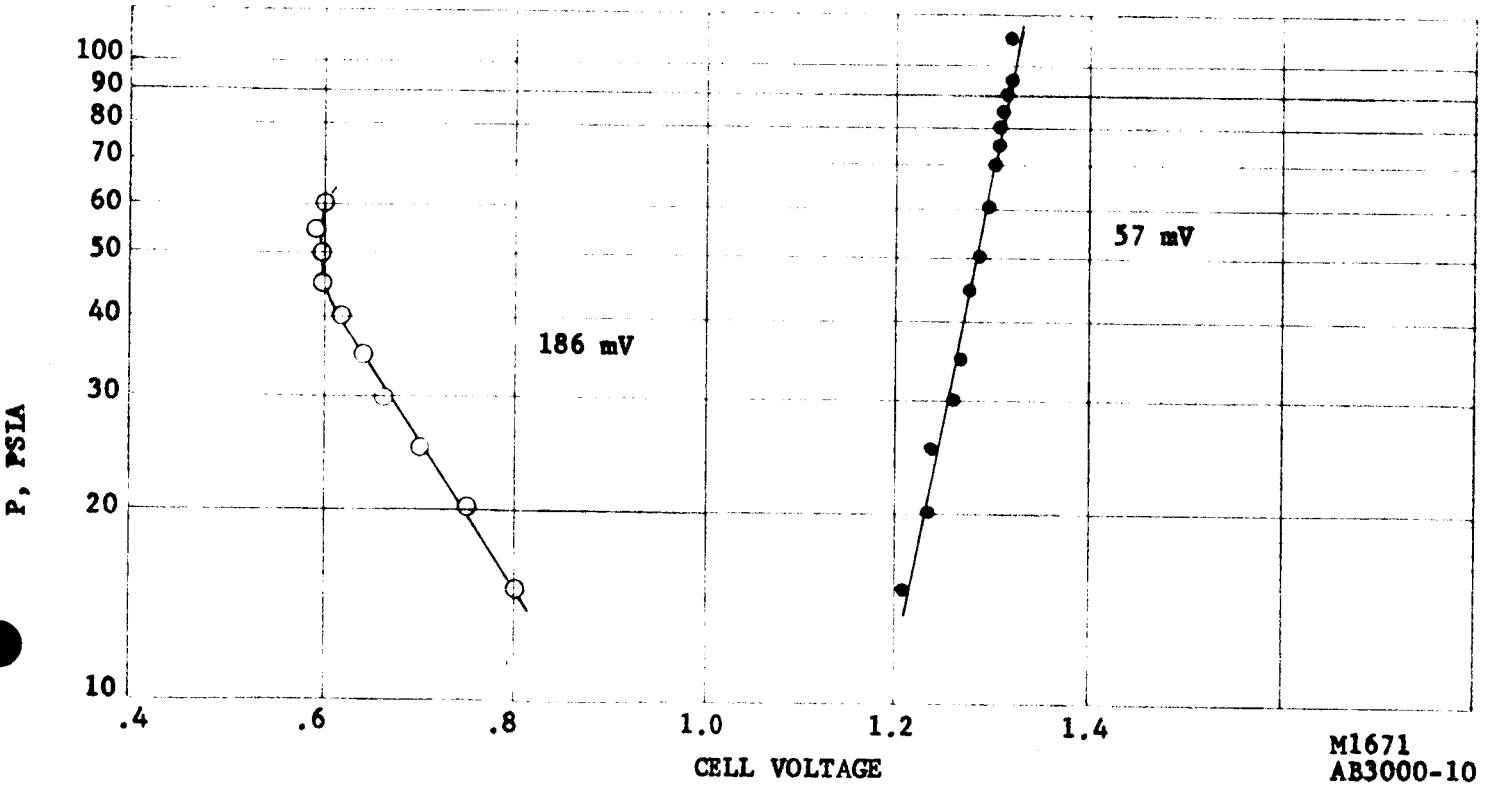

Figure 4 Pressure - Voltage Curves During Oxygen Consumption and Hydrogen Evolution in a Silver-Blank Cell at C/10 Charge Rate - Run No. 2

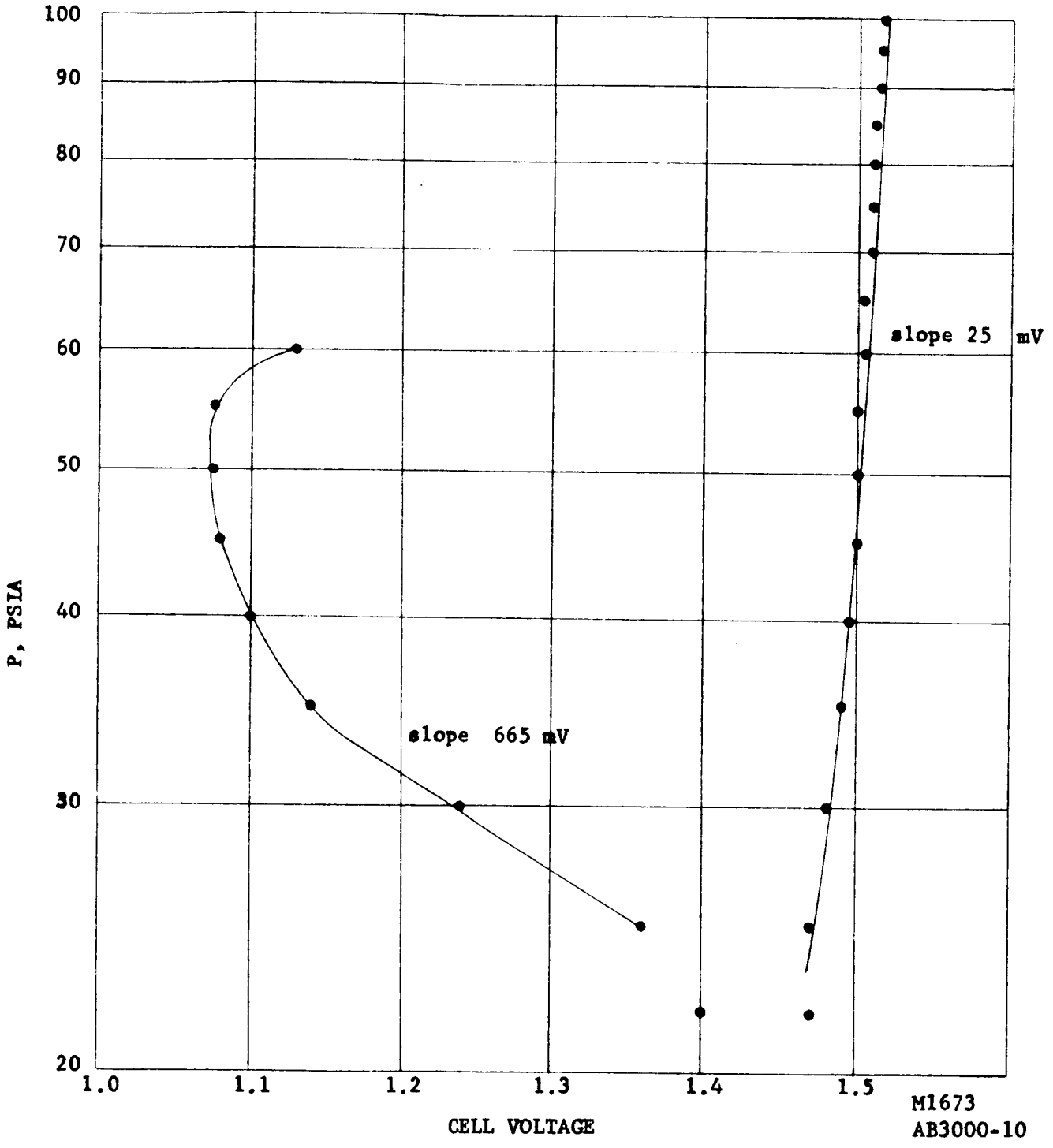

Figure 5 Pressure - Voltage Curves During Oxygen Consumption and Hydrogen Evolution in Nickel-Blank Cells at C/10 Charge Rate - Cell No. 1

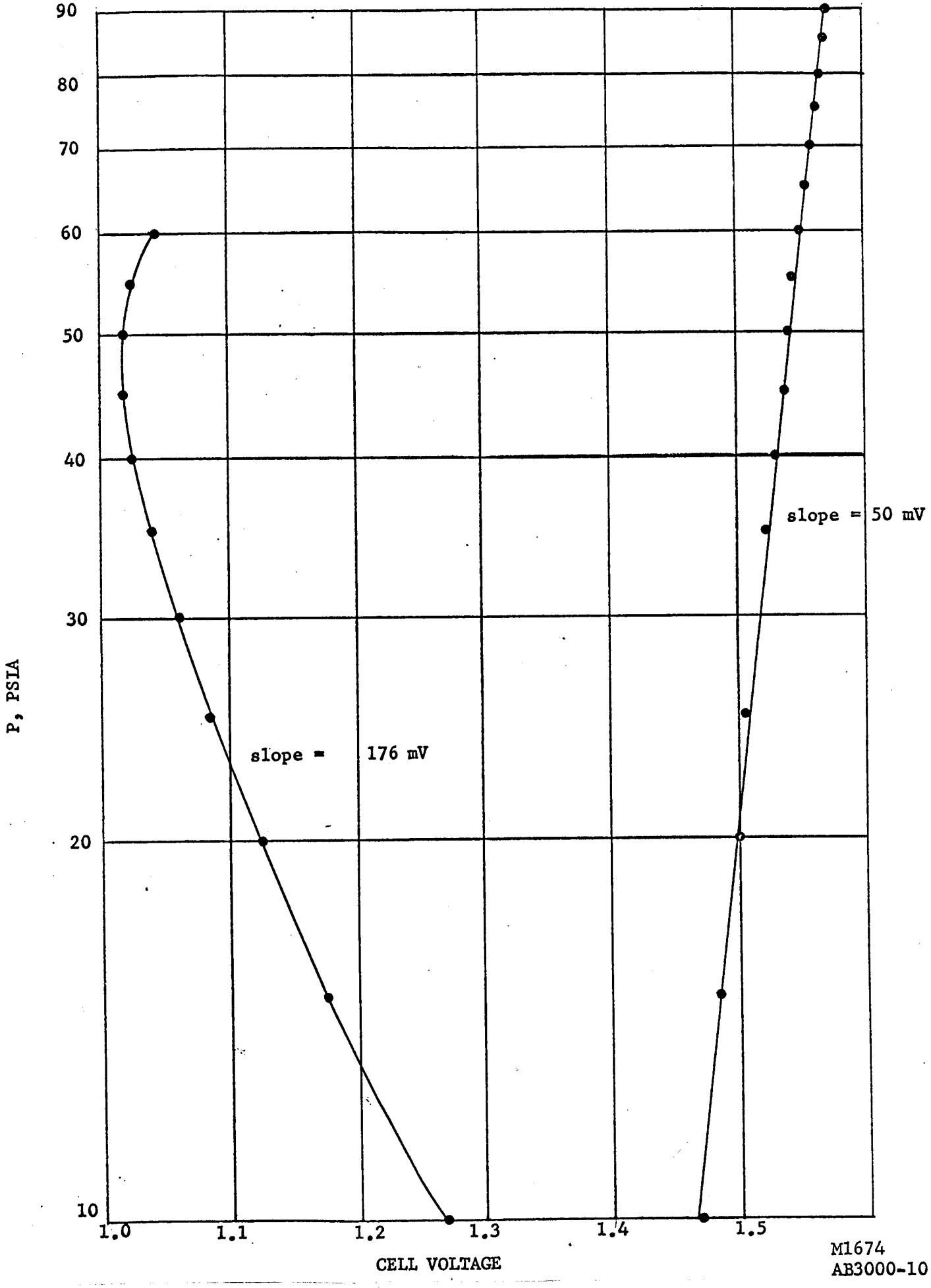

Figure 6 Pressure - Voltage Curves During Oxygen Consumption and Hydrogen Evolution in Nickel-Blank Cells at C/10 Charge Rate - Cell No. 2

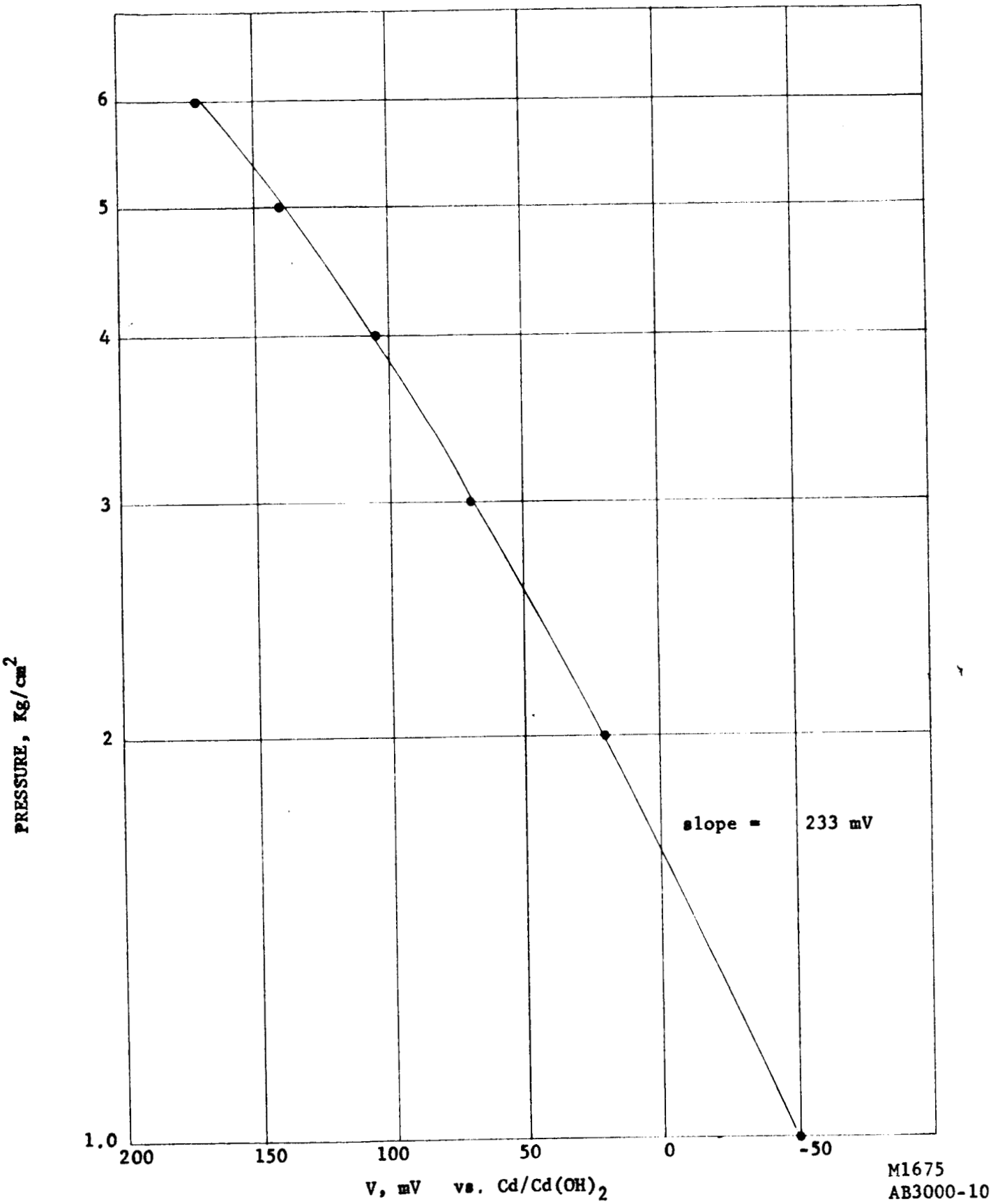

Figure 7 Dehmelt and von Dohren, Proc. Power Sources Conf. 13th Ann., 1959, pp. 85-89. Data taken from Figure 5 at a constant current of 7.5 ma. ($\sim$ C/20)

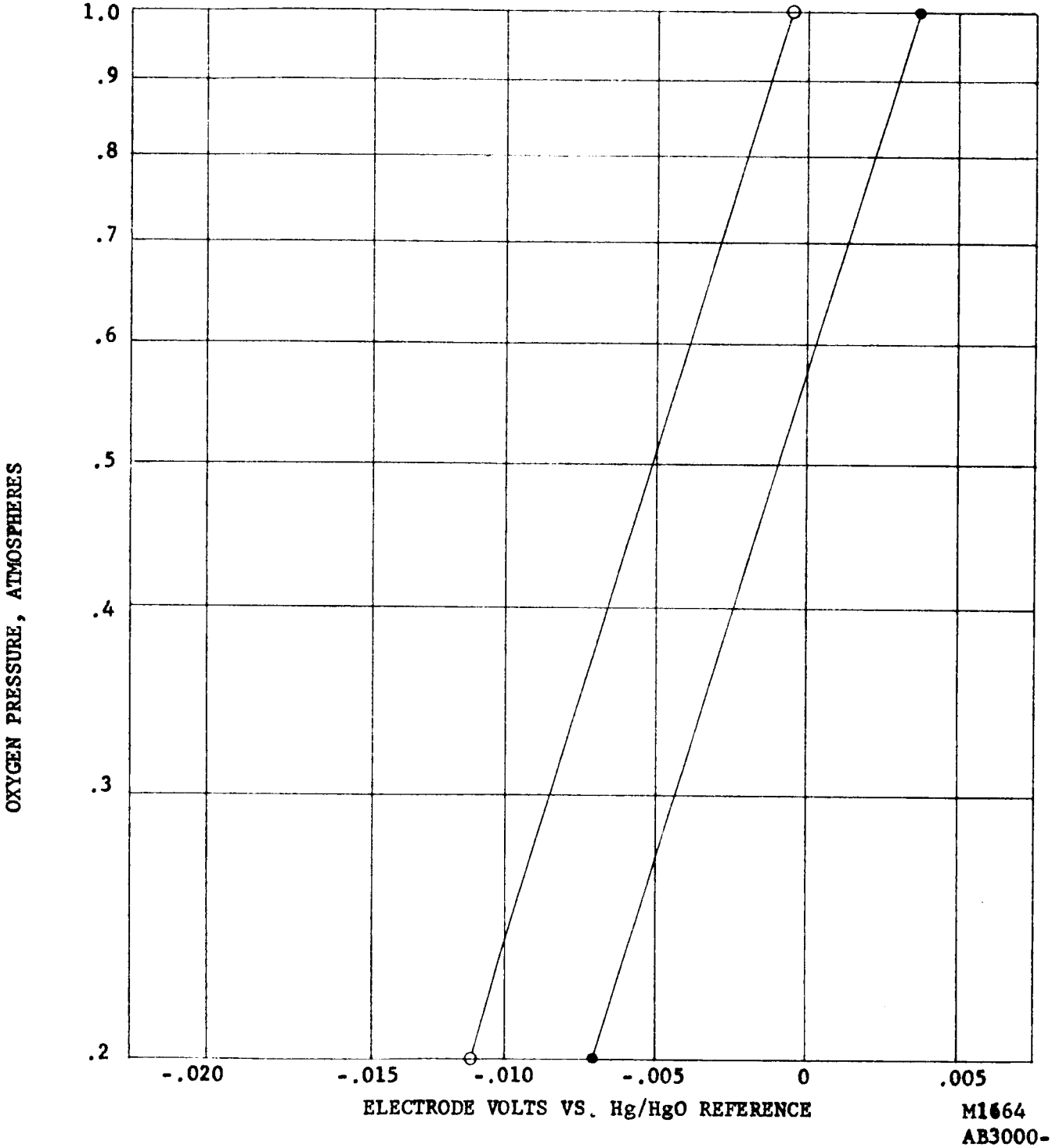

Figure 8 Effect of Pressure on Potential of Selected Hg/HgO - Graphite Pasted Electrodes.

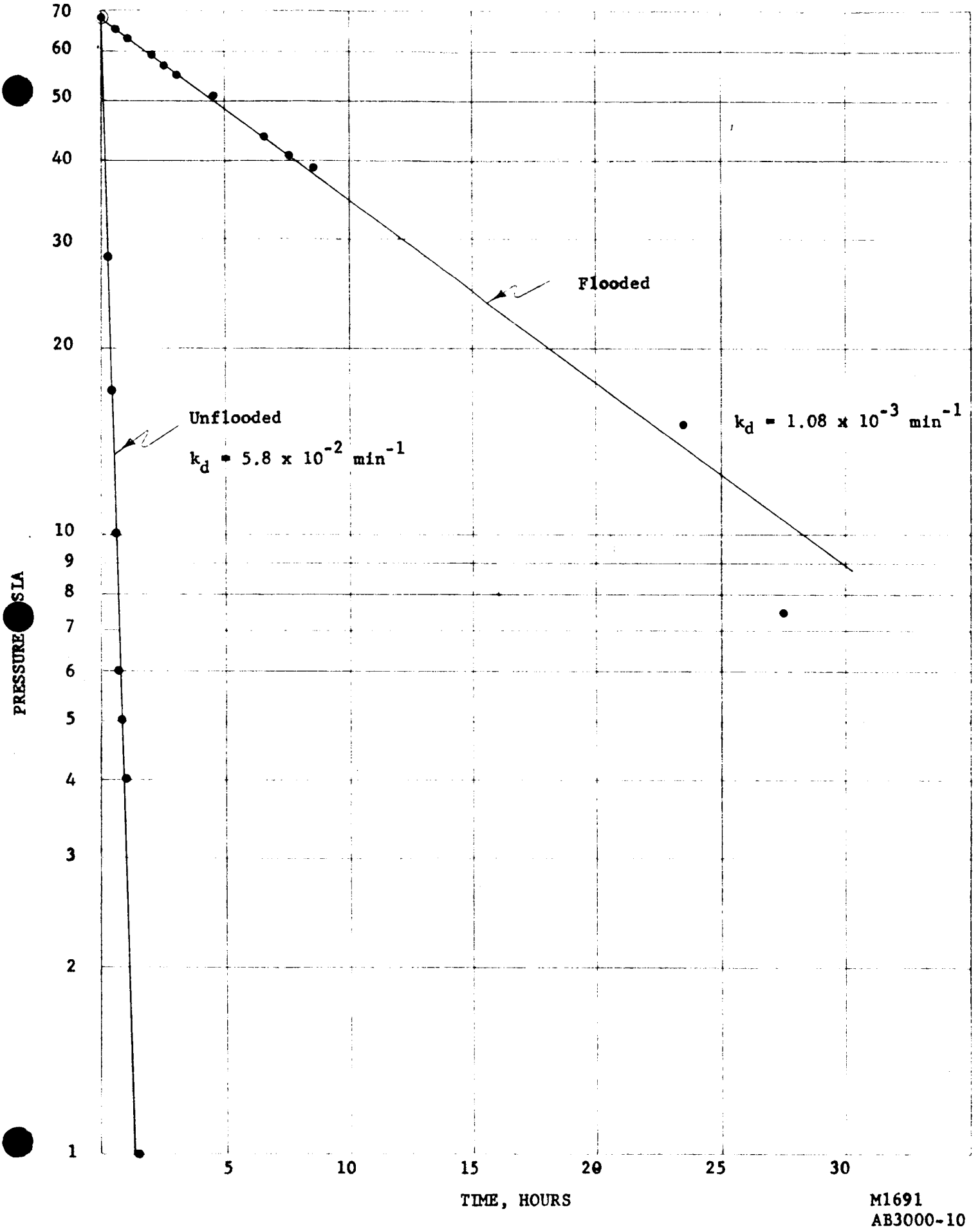

Figure 9 Pressure Decay in Flooded and Non-flooded Cells

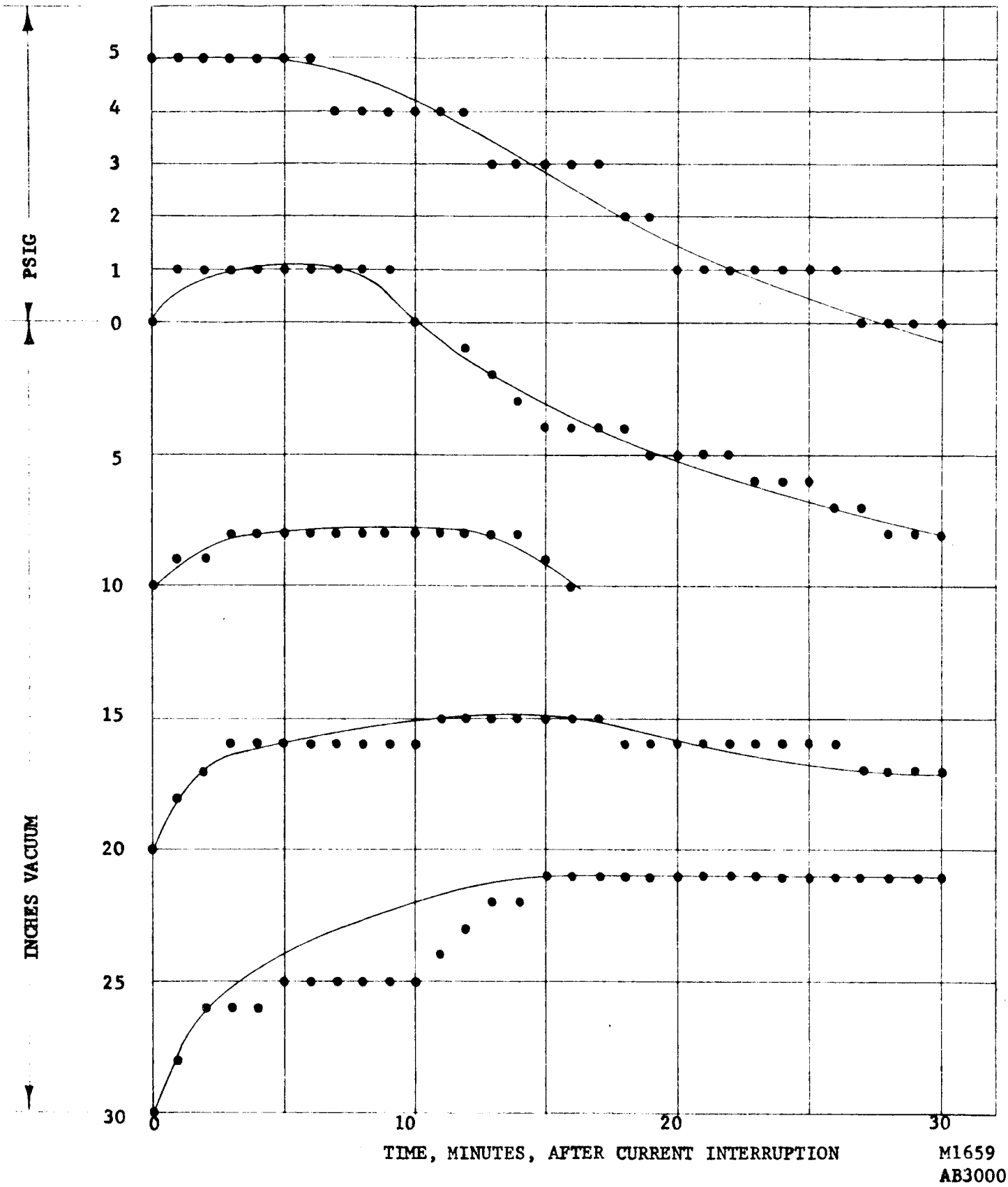

Figure 10 Pressure Changes of Non-flooded VO-6 HS Sealed Nickel-Cadmium Cell at 77°F After 0.6A Charge

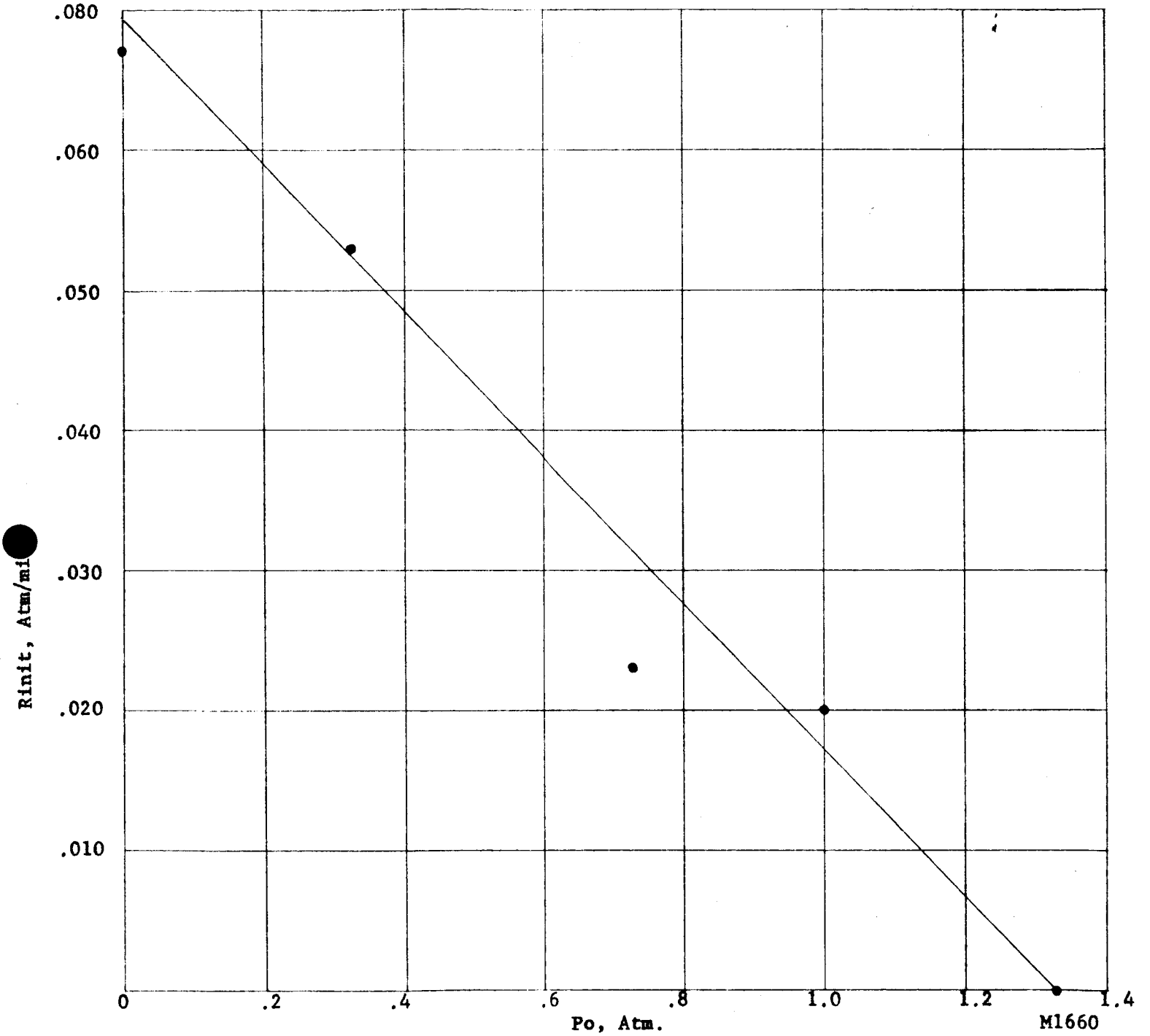

Figure 11 Initial Pressure Rise Vs. Initial Pressure in Non-flooded Sealed Nickel-Cadmium Cell at 77°F

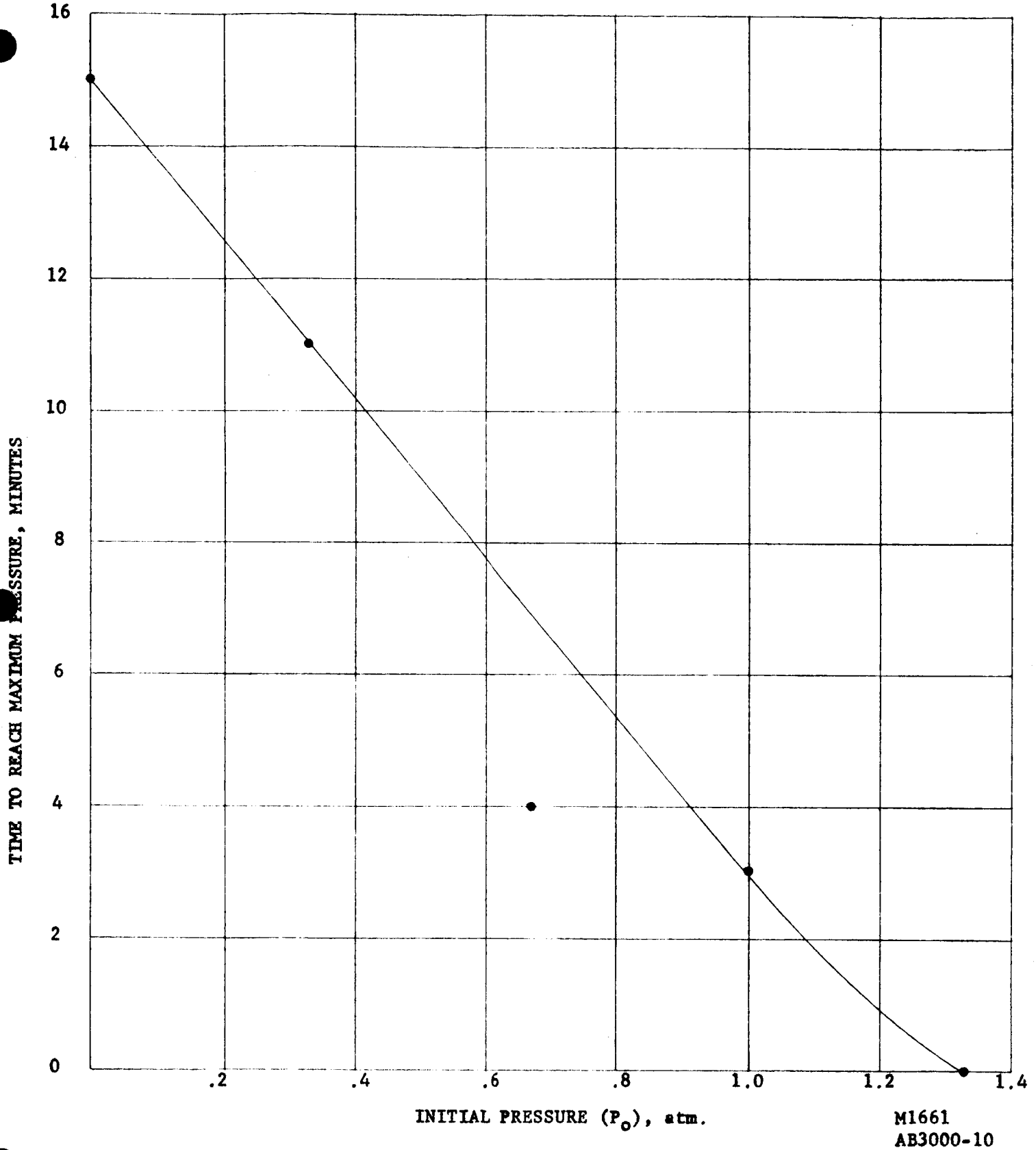

Figure 12 Time for Pressure to Reach a Maximum in a Non-flooded Sealed Nickel-Cadmium Cell at 77°F After a 0.6A Charge

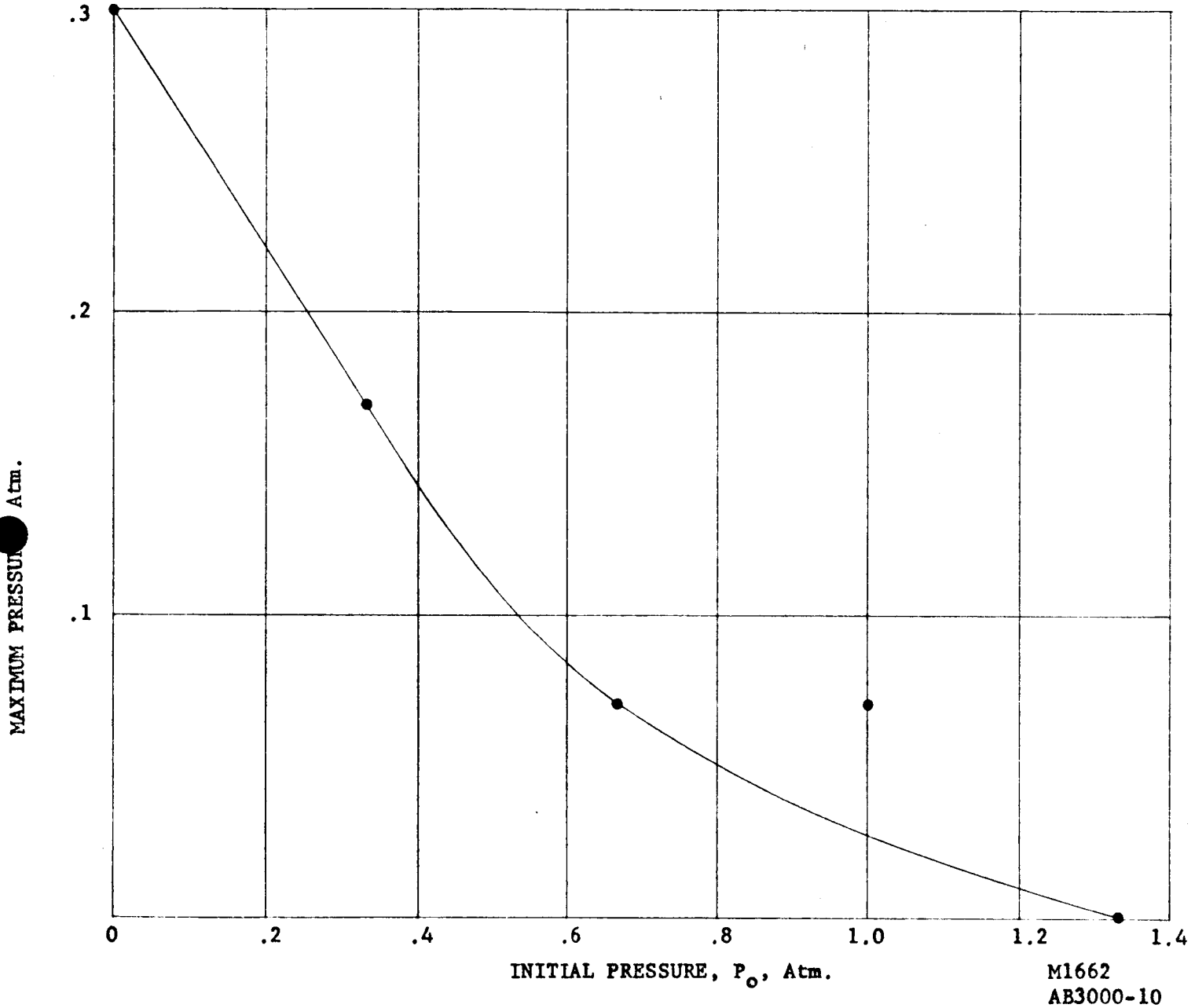

Figure 13 Maximum Pressure Rise in a Non-flooded Sealed Nickel-Cadmium Cell at 77°F After a 0.6A Charge

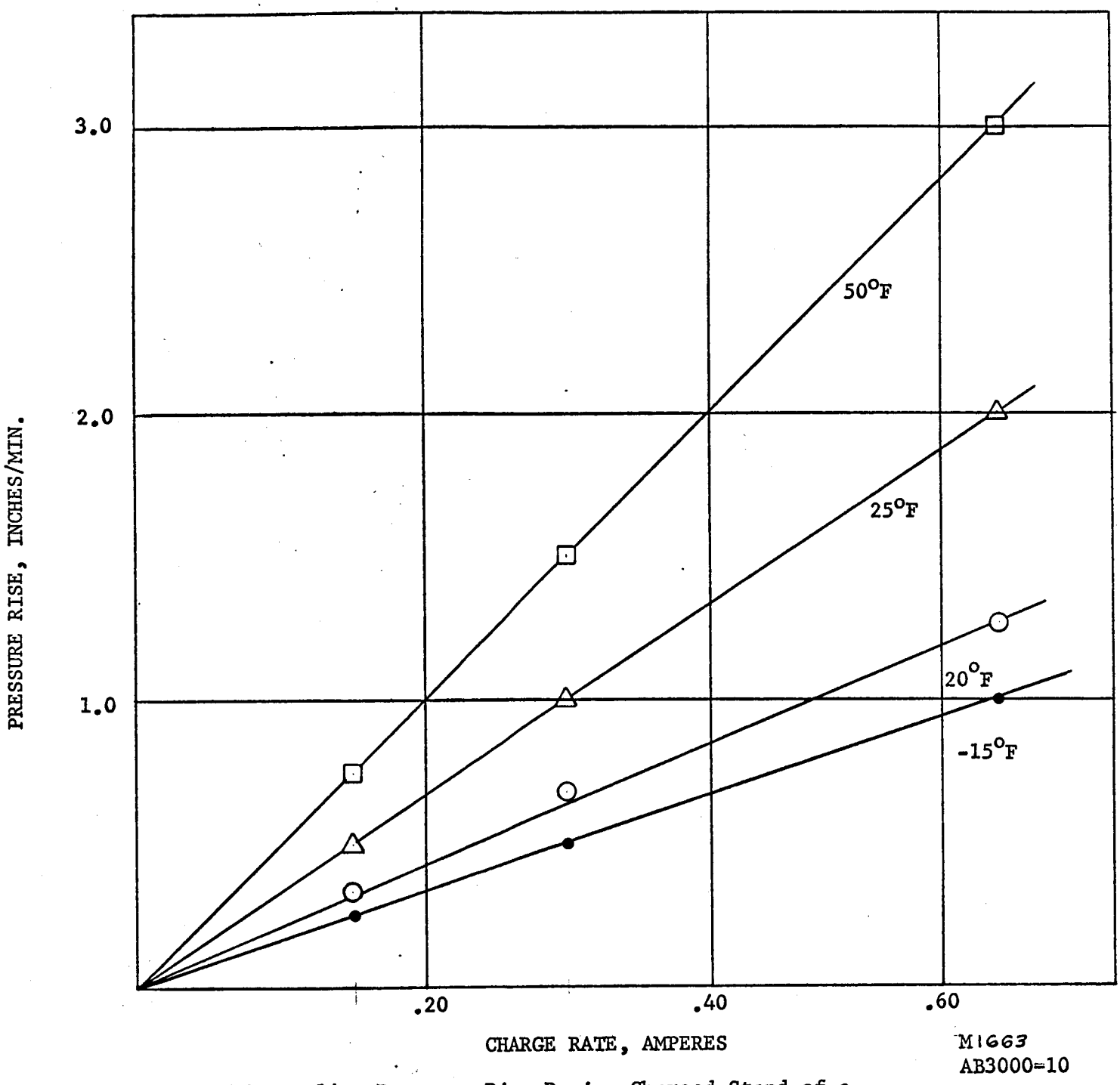

Figure 14 Pressure Rise During Charged Stand of a Non-flooded Sealed Nickel-Cadmium Cell

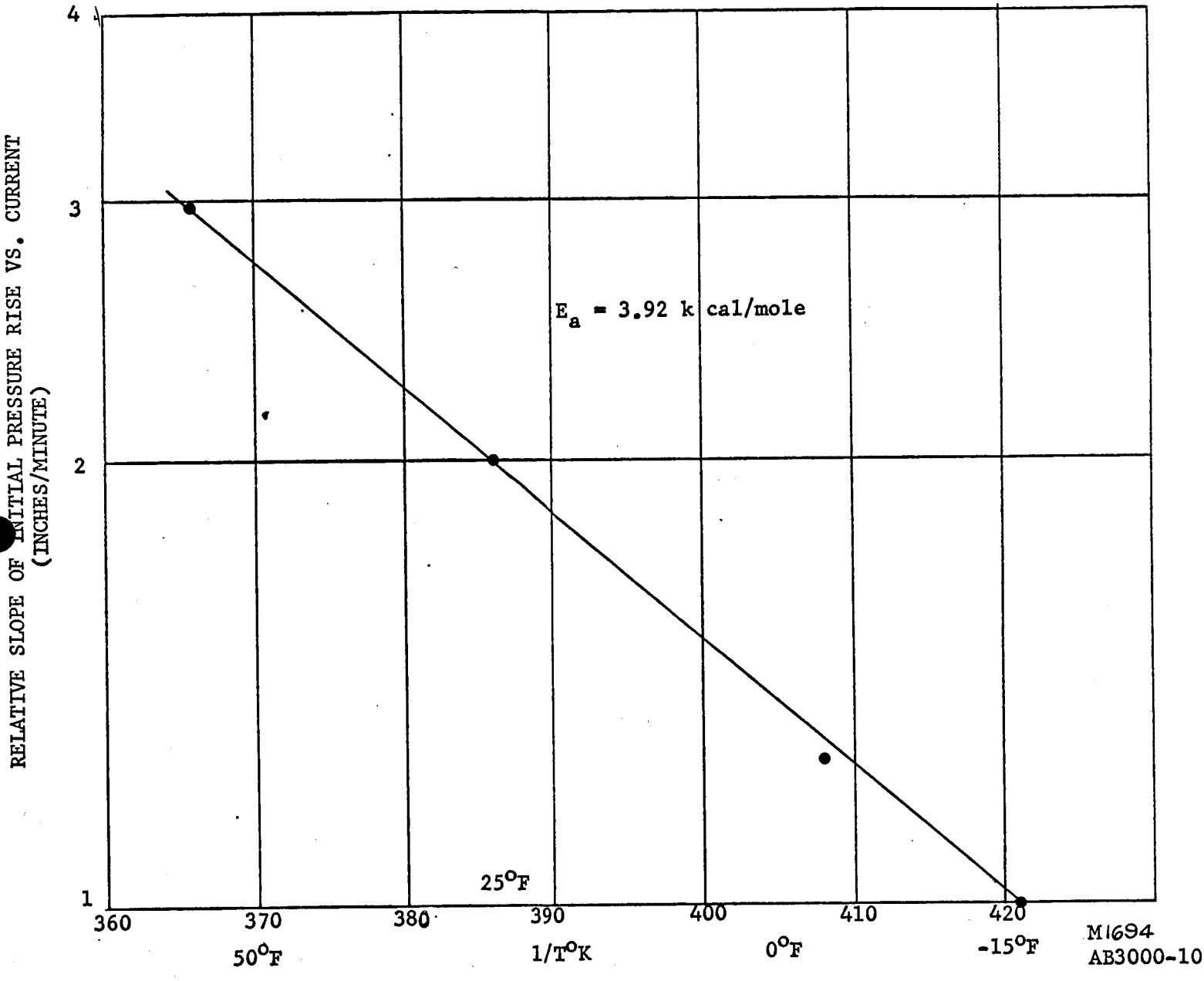

Figure 15 Slope of Decay Rate Vs. Current as a Function of Temperature in a Non-flooded Sealed Nickel-Cadmium Cell

Figure 16 Pressure Rise in a Flooded VO 6-HS Nickel-Cadmium Cell at 77°F After 0.6A Charge for Two Hours.

M1665

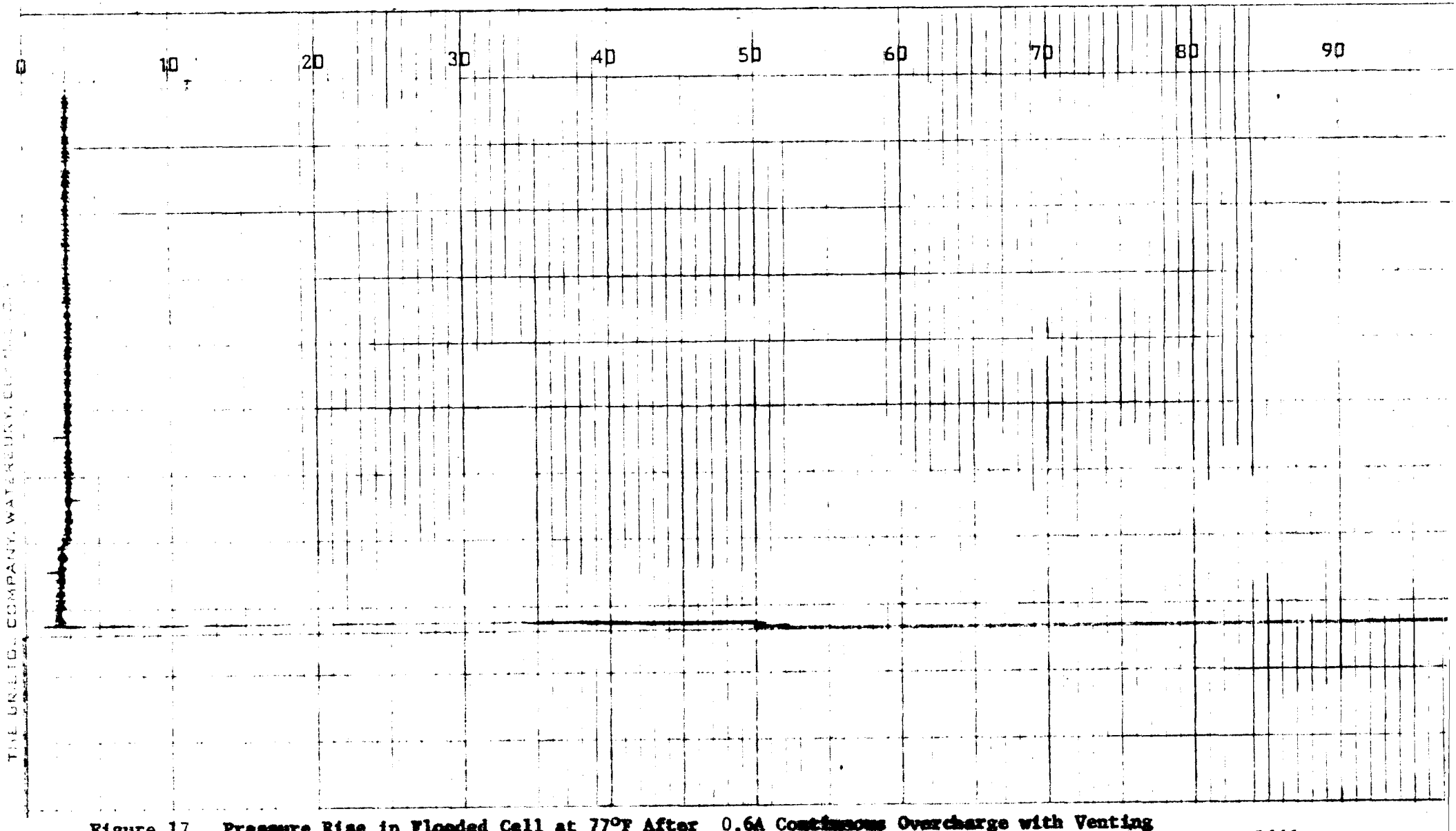

Figure 17 **Pressure Rise in Flooded Cell at 77°F After 0.6A Continuous Overcharge with Venting**

M1666
AB3000-10

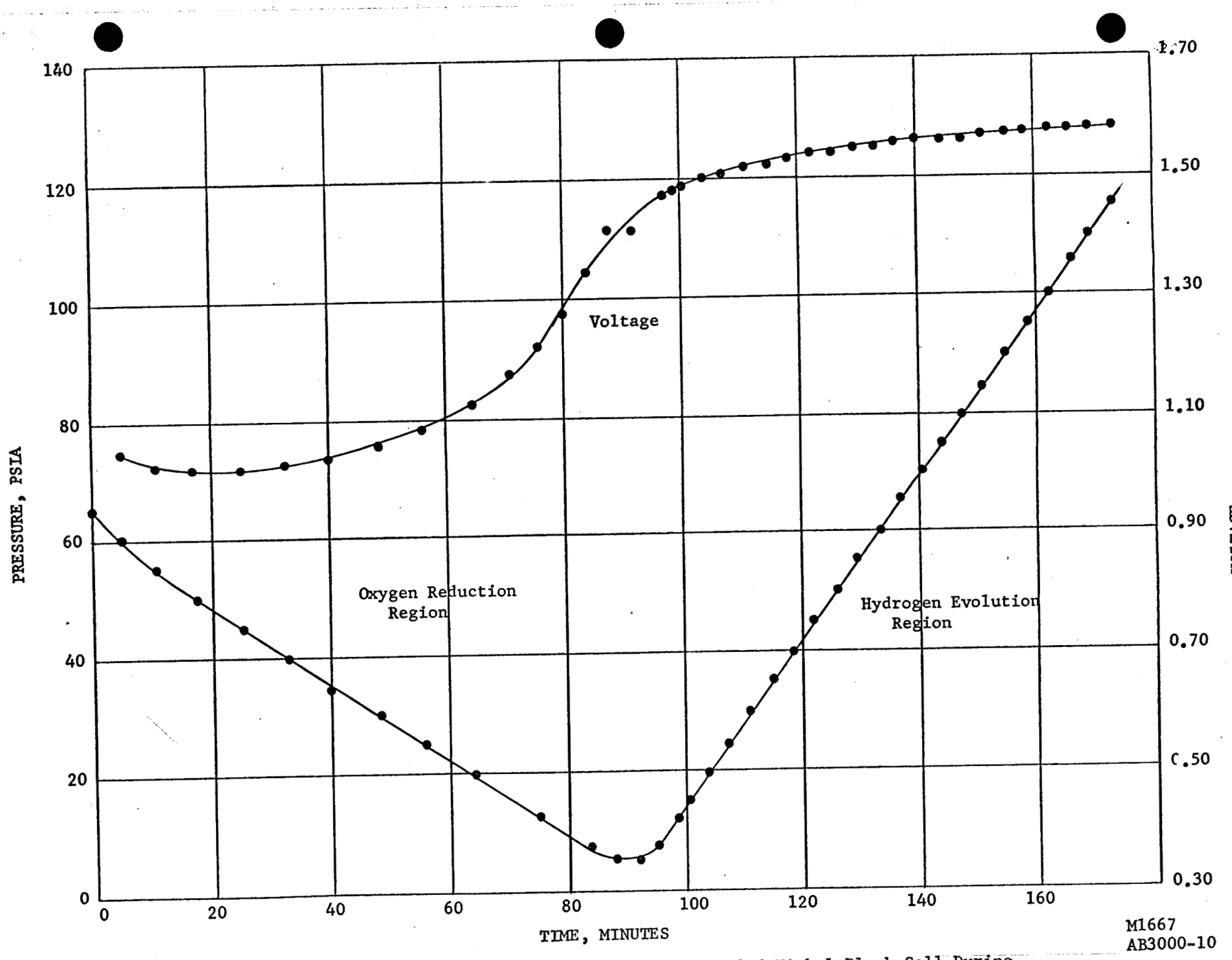

Figure 18 Pressure and Voltage Changes in a Sealed Nickel-Blank Cell During Charge at 0.6A After Pressurization with 50 psig Oxygen

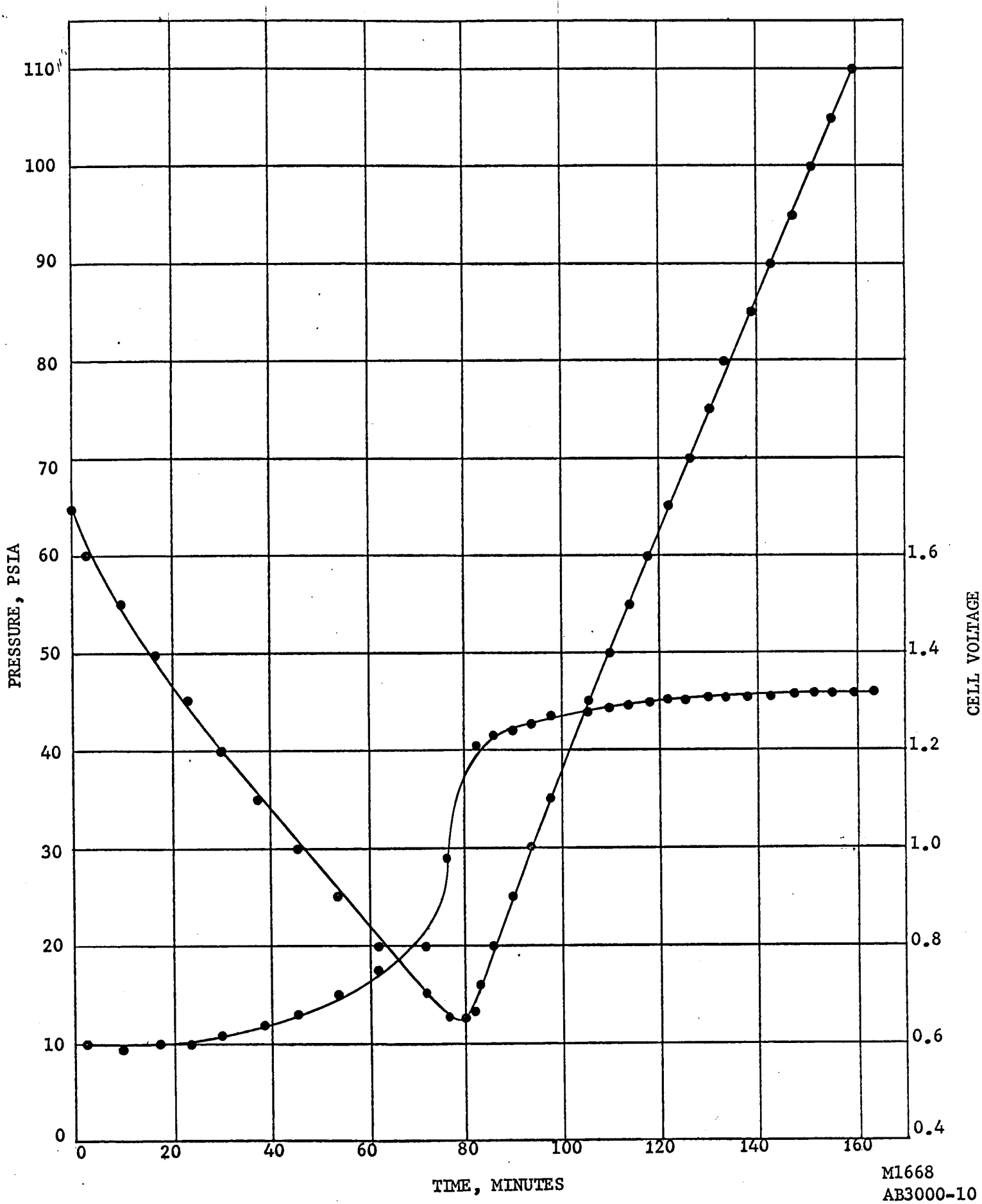

Figure 19 Pressure and Voltage Changes in a Sealed Silver-Blank Cell During Charge at 0.6A After Pressurization with 50 psig Oxygen

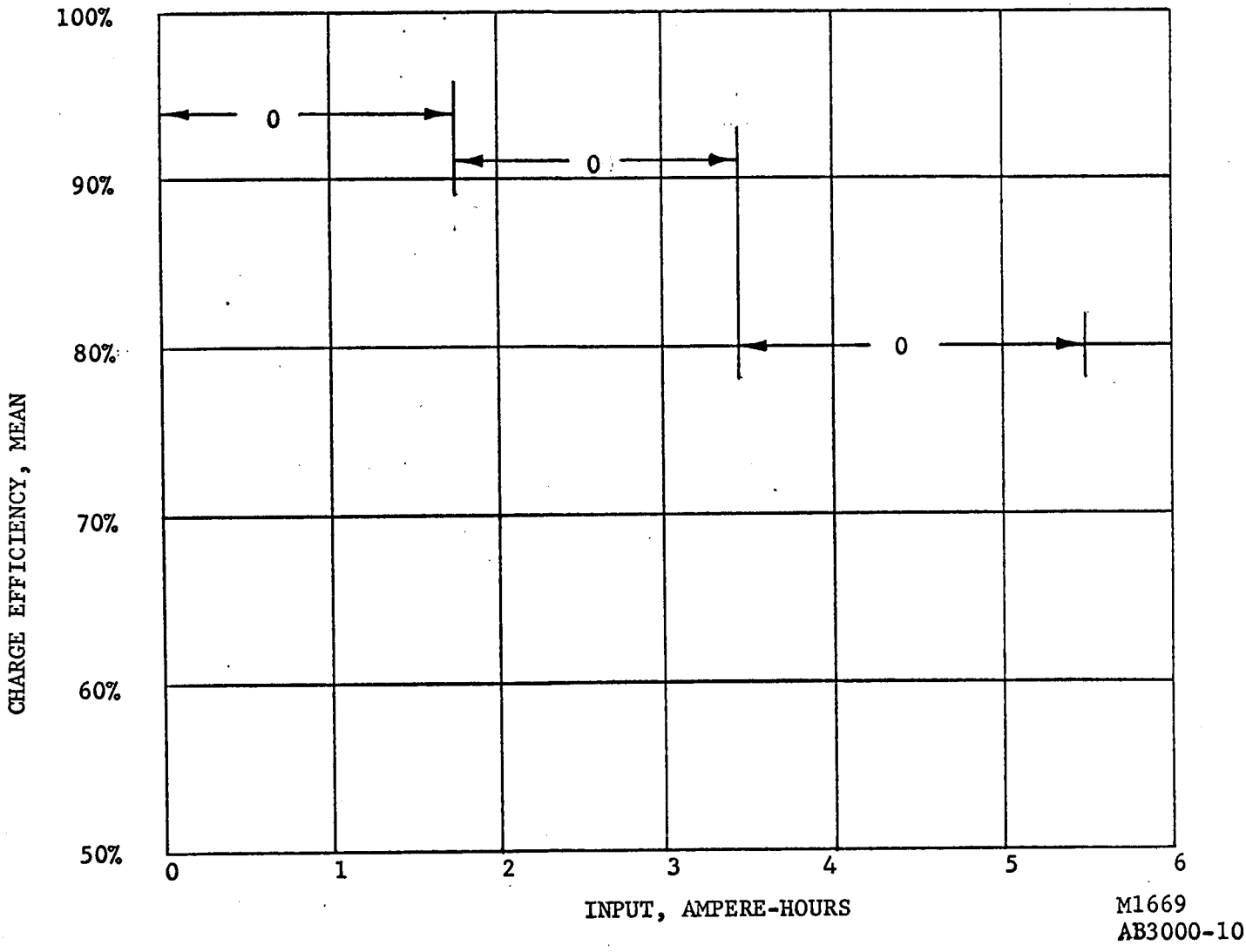

Figure 20 Mean Charge Efficiency of VO-6 HS Cells as a Function of Charge Input

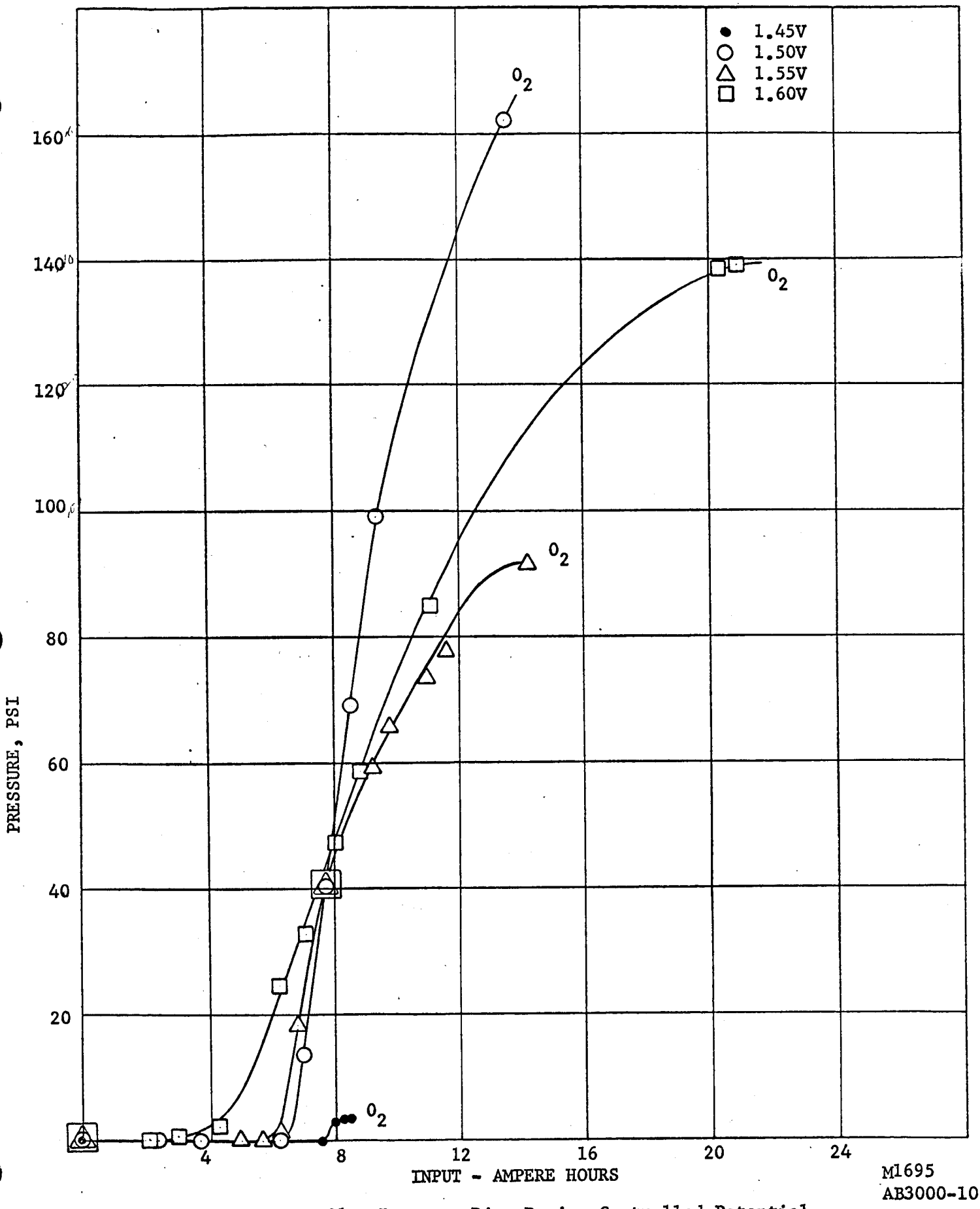

M1695
AB3000-10

Figure 21 Pressure Rise During Controlled Potential Charge of VO-6 HS Cells at 50°F

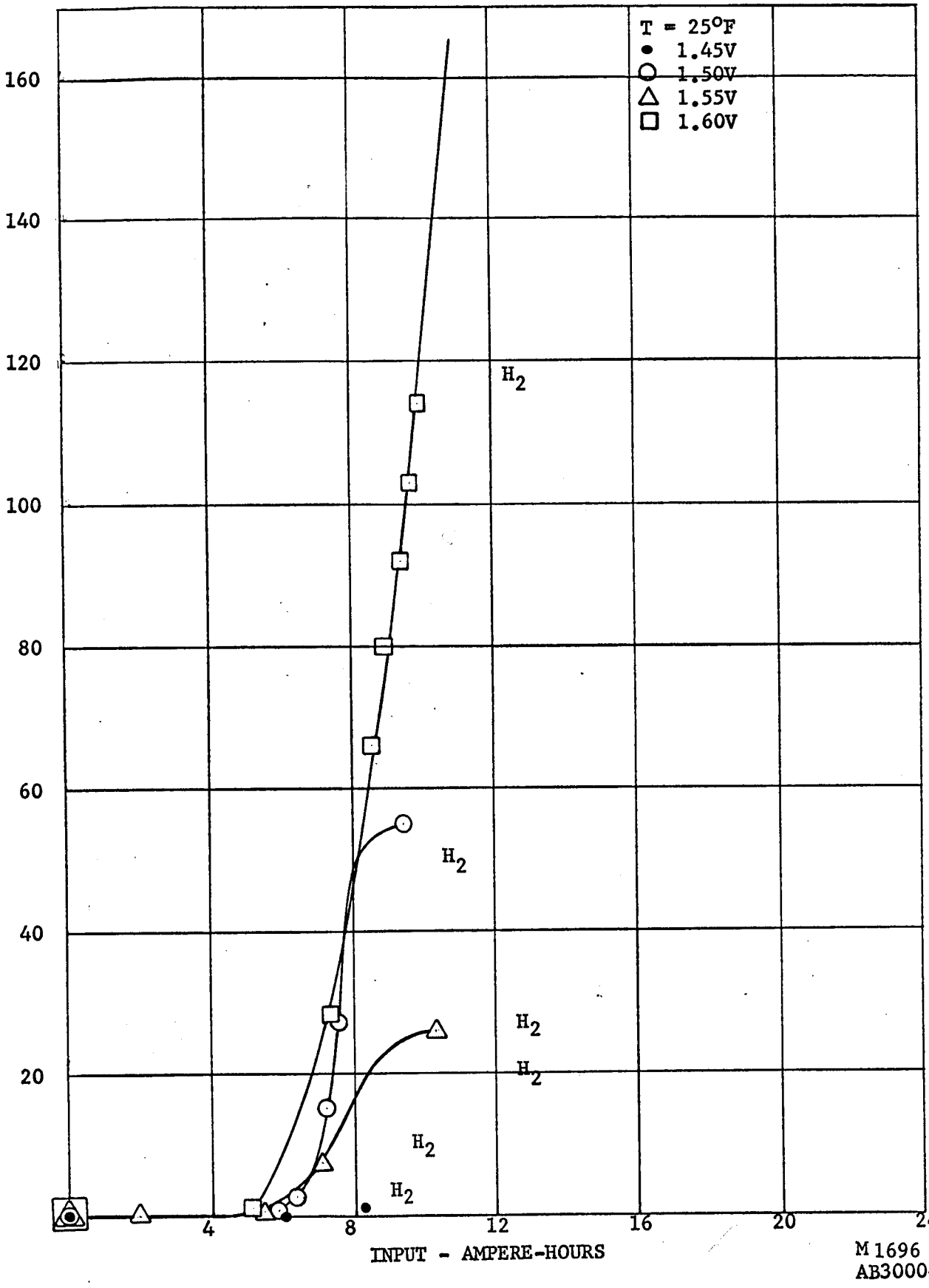

Figure 22 Pressure Rise During Controlled Potential Charge of VO-6 HS Cells at 25°F

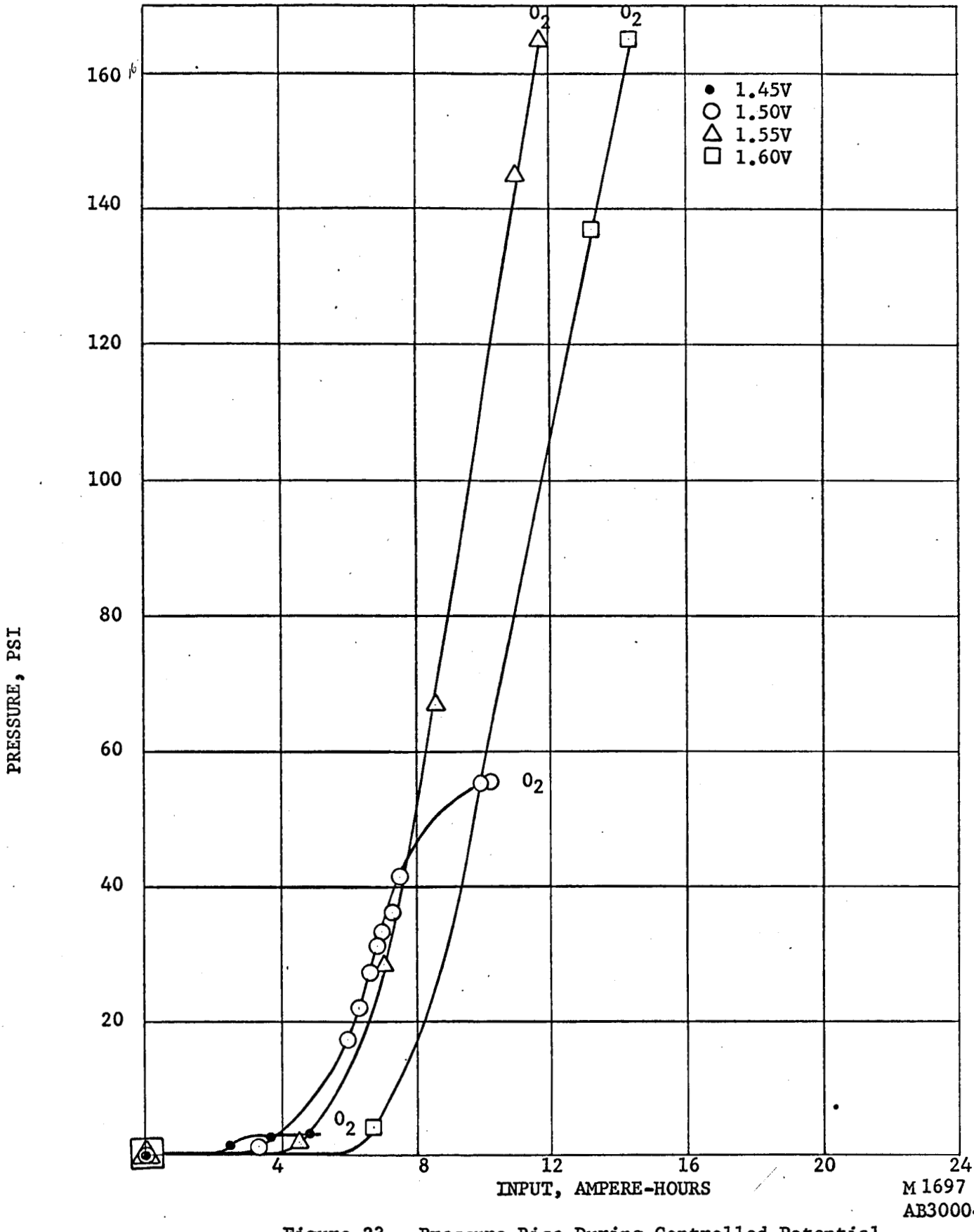

Figure 23 Pressure Rise During Controlled Potential Charge of VO-6 HS Cells at 0°F

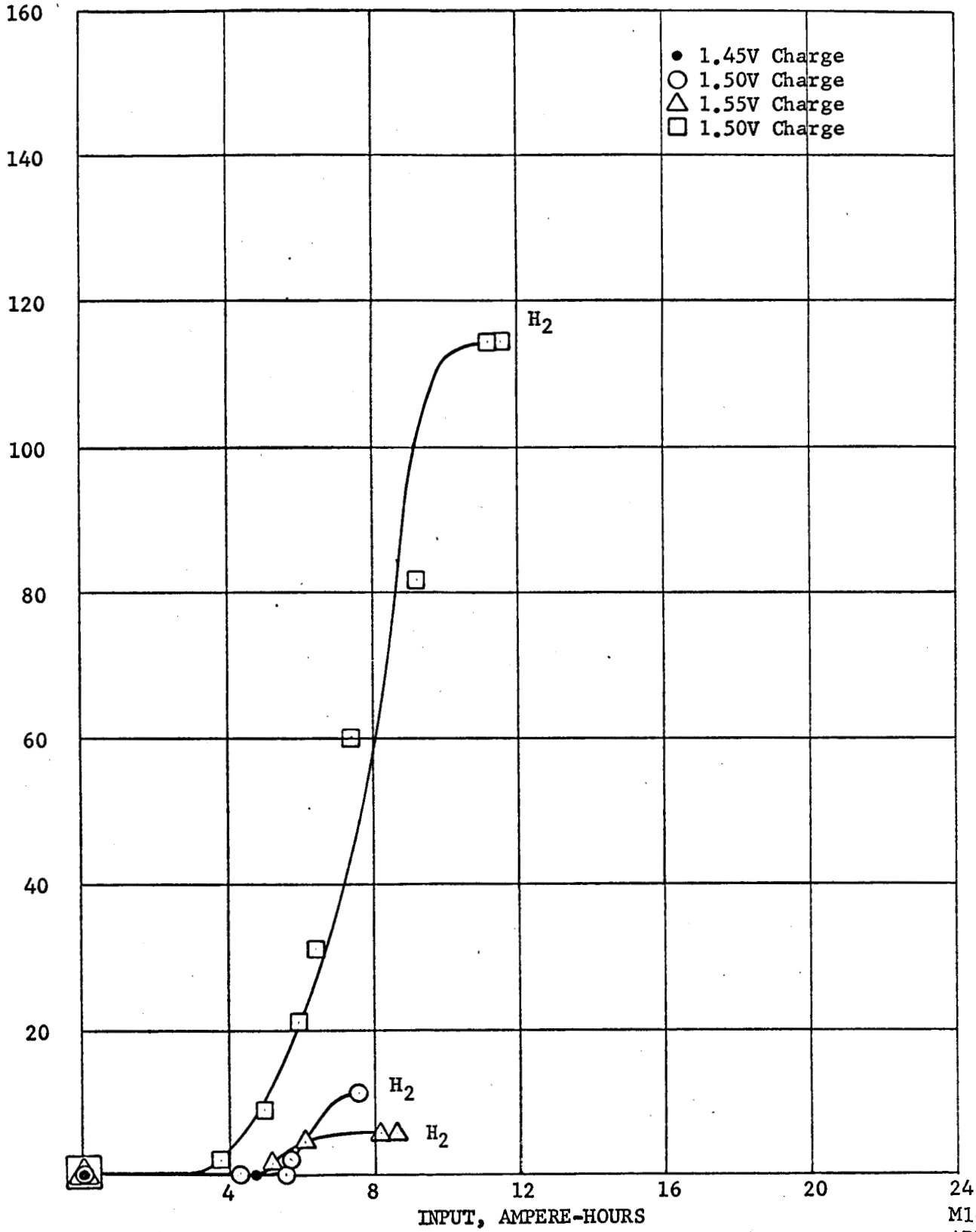

M1698
AB3000-10

Figure 24 Pressure Rise During Controlled Potential Charge of VO-6 HS Cells at -15°F

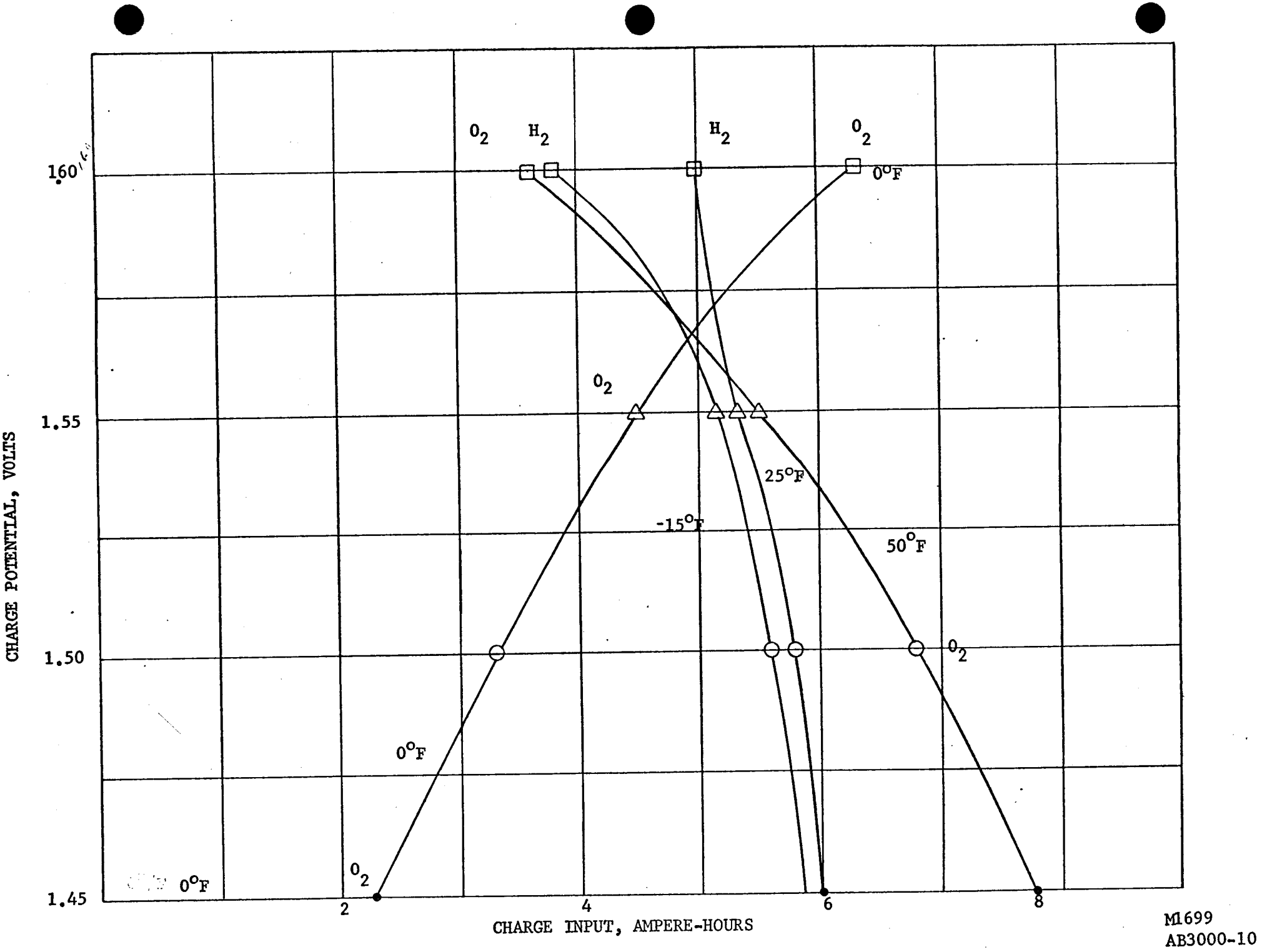

Figure 25 Charge Input to Start Pressure Rise in VO-6 HS Cells at Various Temperatures

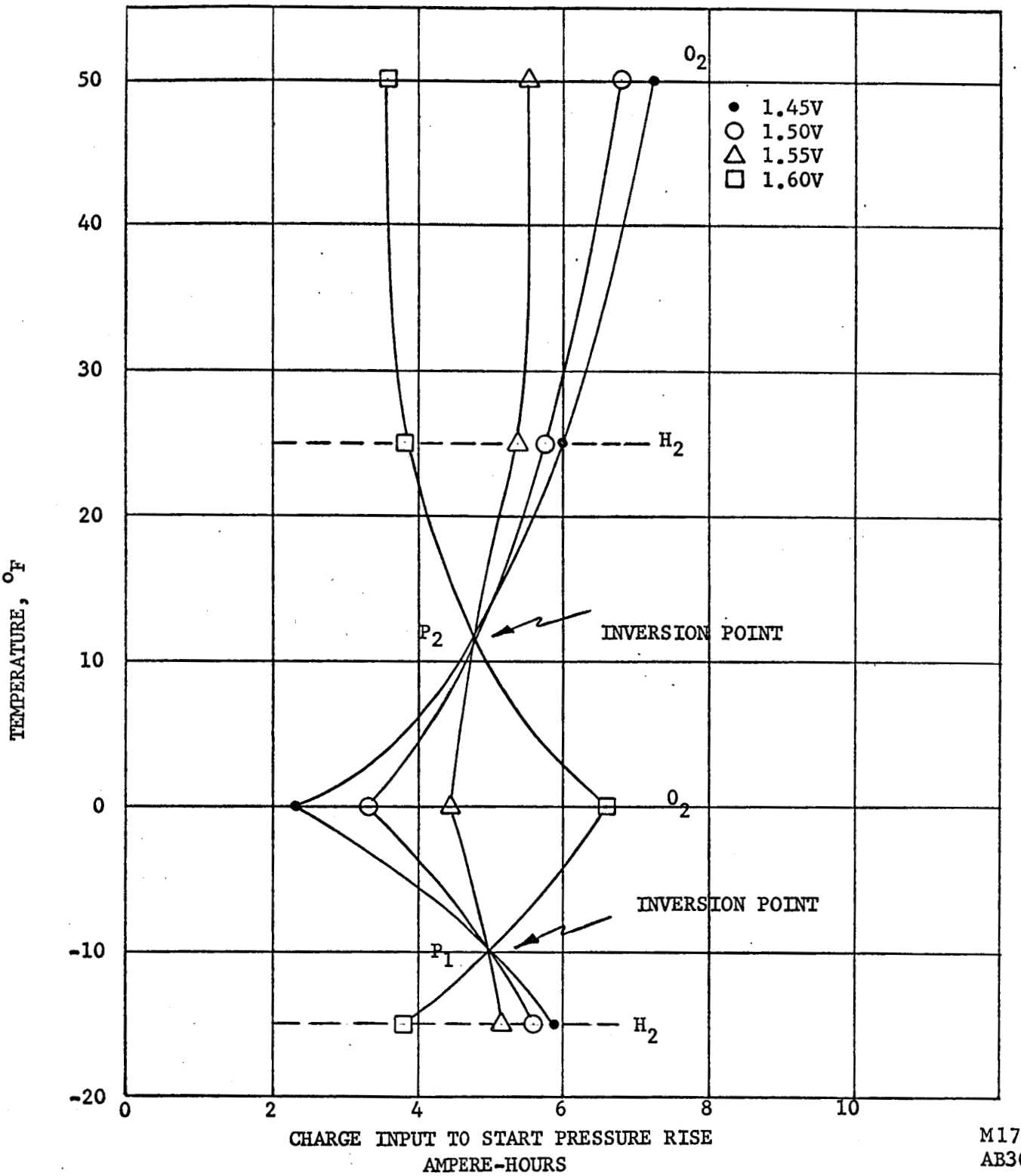

Figure 26 Charge Input to Start Pressure Rise in VO-6 HS Cells at Various Potentials

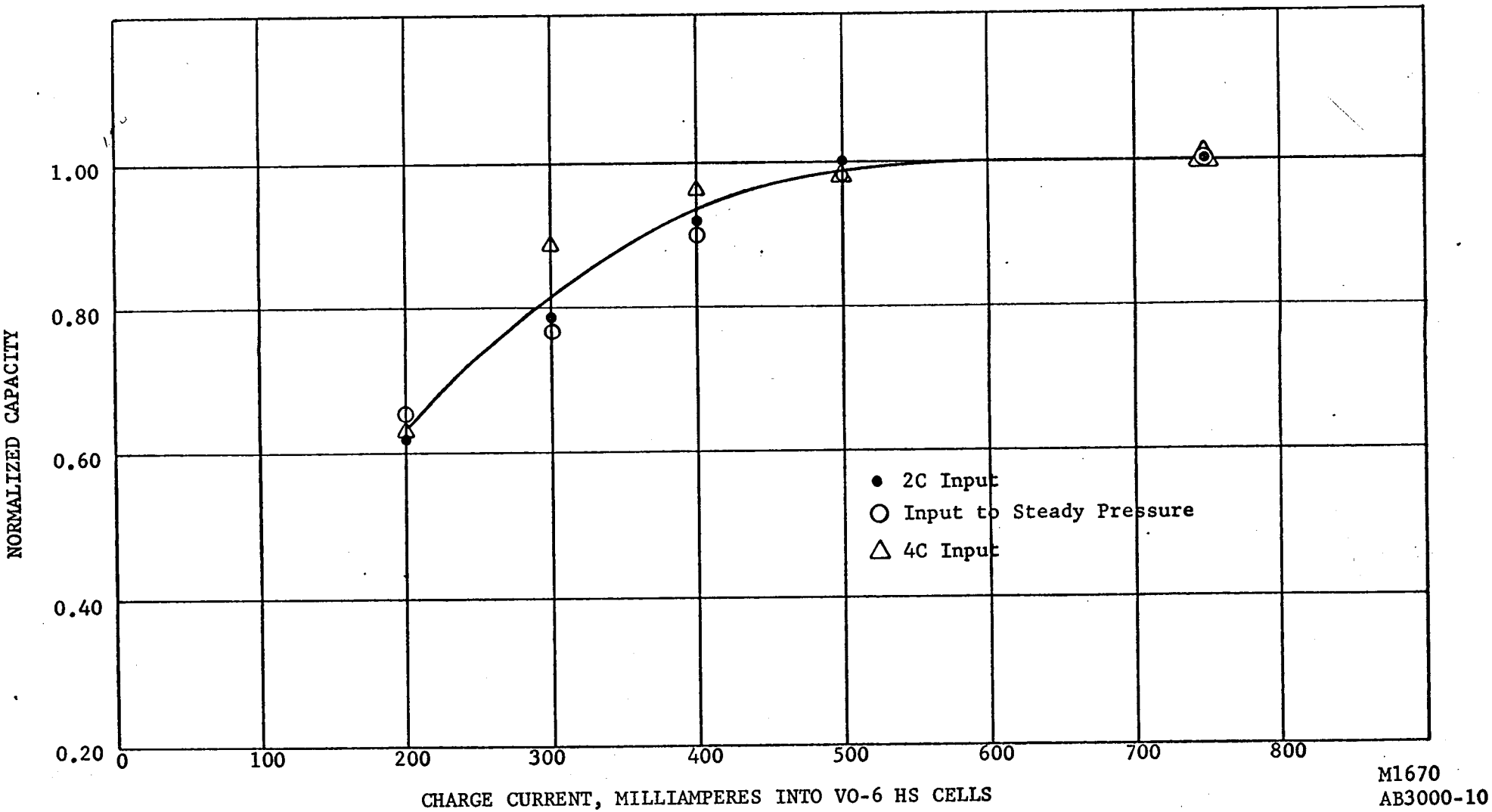

Figure 27 Normalized Capacity of VO-6 HS Cells Following Charge at Various Rates

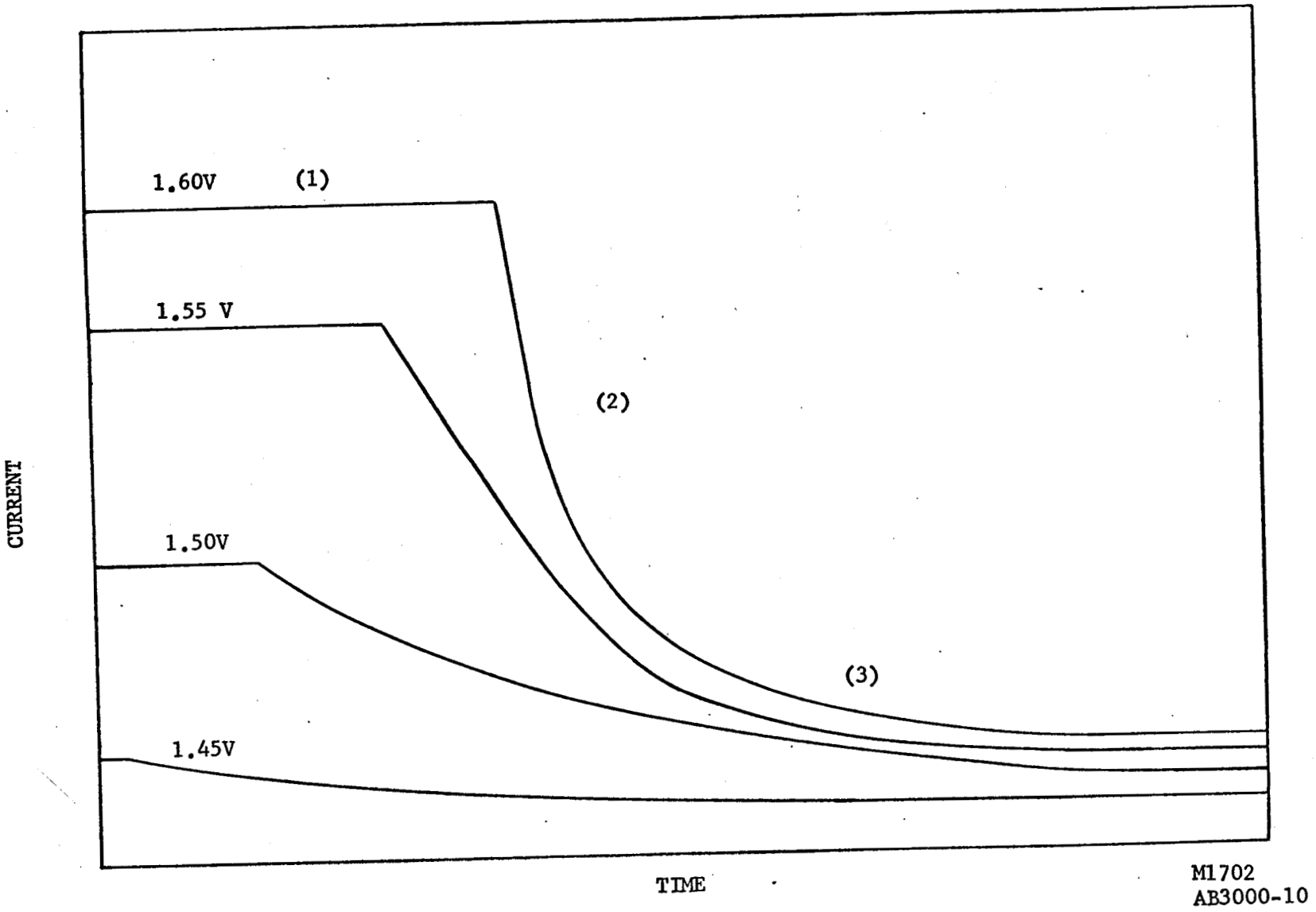

Figure 28 Typical Set of Current Vs. Time Curves Obtained During Constant Potential Charges at any Temperature

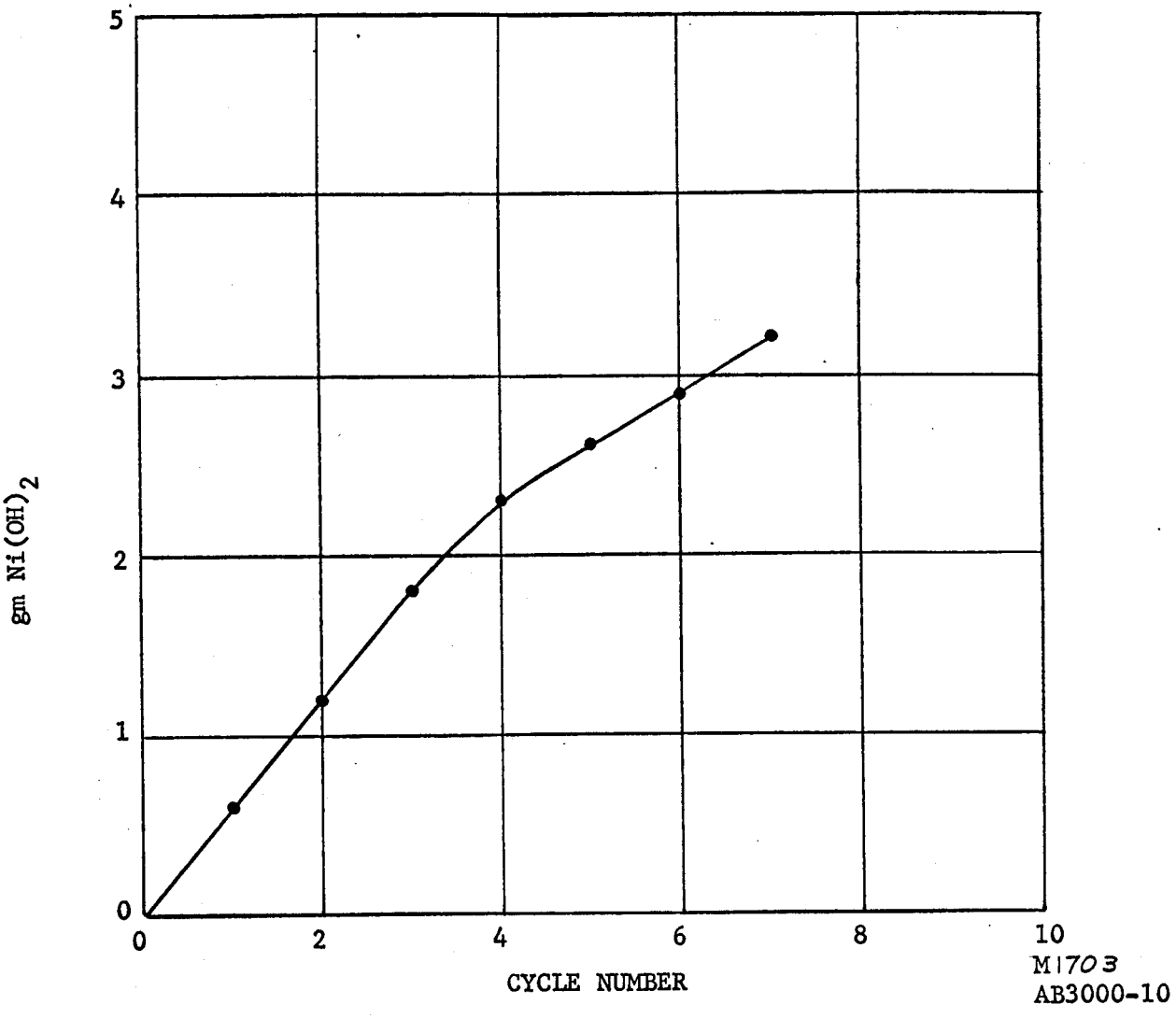

Figure 29 Weight Gains of Positive Plates

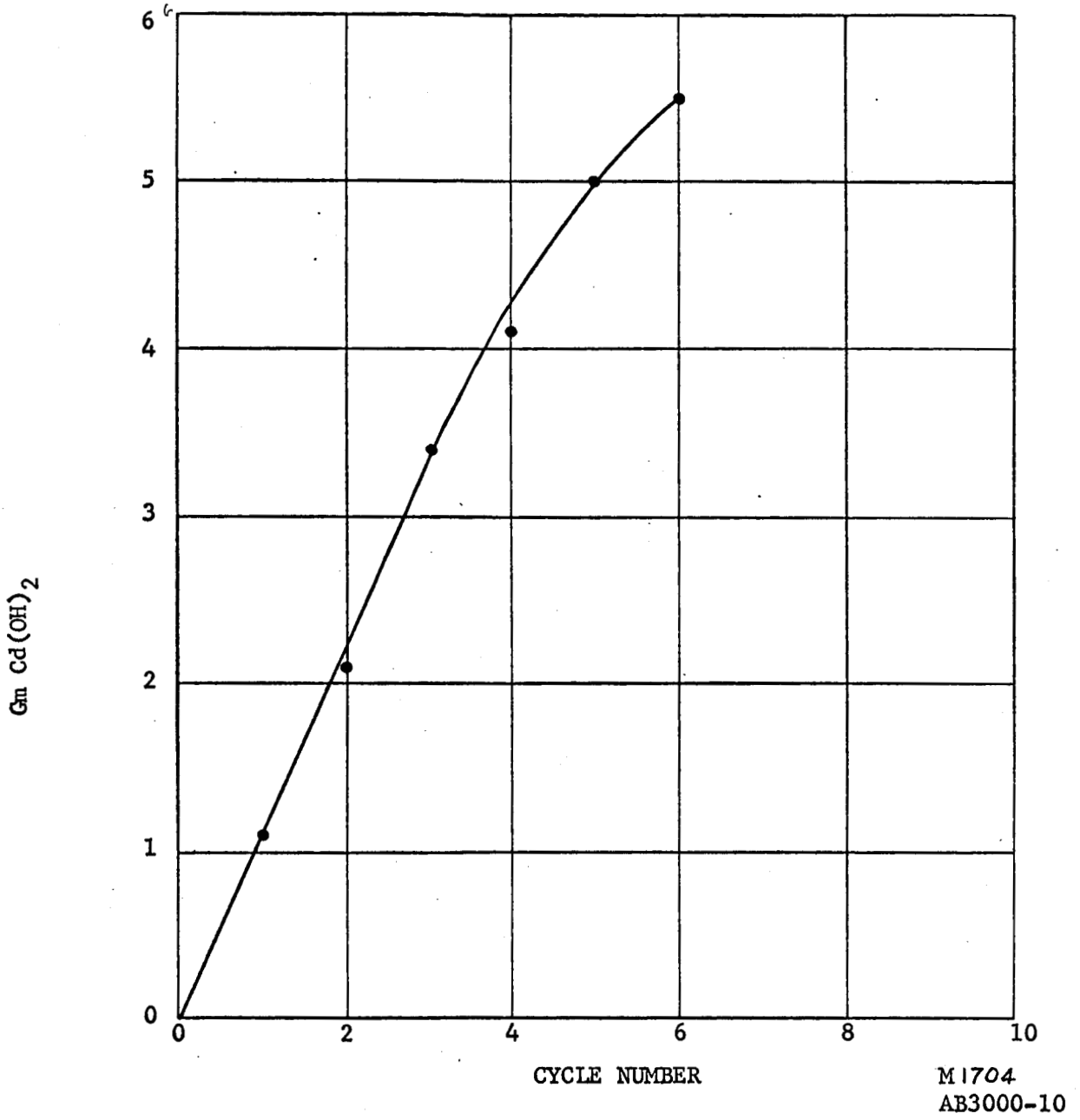

Figure 30 Weight Gains of Negative Plates

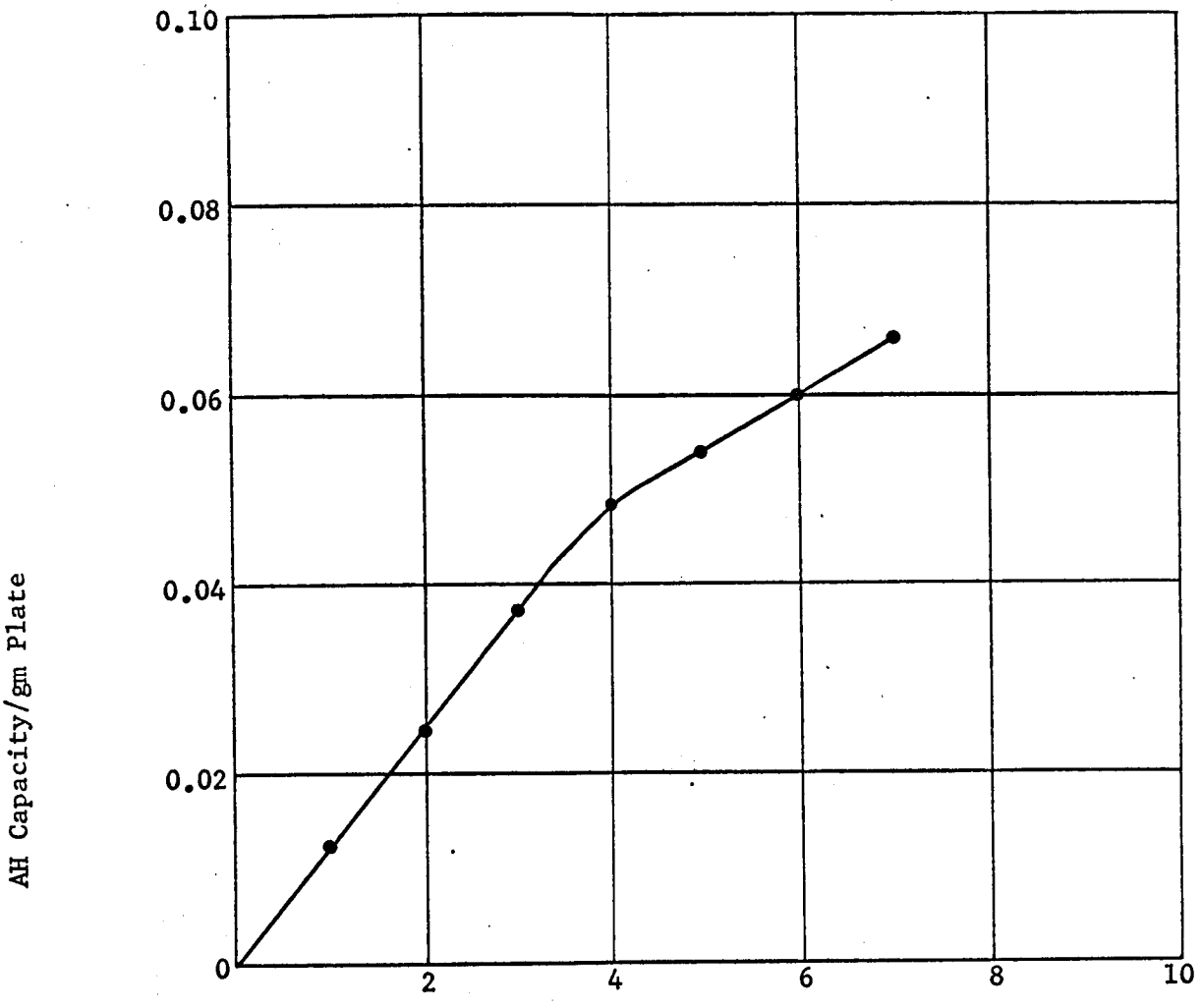

Figure 31 Ampere-Hour Capacity Gains as a Function of Impregnation Cycles